on the proteasomal pathways: 20S ubiquitin-independent, 26S ubiquitin-indenedent and 26S ubiquintin-dependent. Program No.132.8. Abstract viewer/Itinerary Planner. Society for Neuroscience, Washinton, DC, 2003.

[35] A. Takeda, M. Mallory, M. Sundsmo, W. Honer, L. Hansen, E. Masliah, Abnormal accumulation of NACP/alpha-synuclein in neurodegenerative disorders, Am. J. Pathol. 152 (1998) 367–372.

[36] A. Takeda, M. Hashimoto, M. Mallory, M. Sundsumo, L. Hansen, E. Masliah, C-terminal alpha-synuclein immunoreactivity in structures other than Lewy bodies in neurodegenerative disorders, Acta Neuropathol. (Berl.) 99 (2000) 296–304.

[37] P.H. Tu, J.E. Galvin, M. Baba, B. Giasson, T. Tomita, S. Leight, S. Nakajo, T. Iwatsubo, J.Q. Trojanowski, V.M. Lee, Glial cytoplasmic inclusions in white matter oligodendrocytes of multiple system atrophy brains contain insoluble alpha-synuclein, Ann. Neurol. 44 (1998) 415–422.

[38] K.D. Wilkinson, S. Deshpande, C.N. Larsen, Comparisons of neuronal (PGP 9.5) and non-neuronal ubiquitin C-terminal hydrolases, Biochem. Soc. Trans. 20 (1992) 631–637.

[39] D. Willwohl, M. Kettner, H. Braak, G.B. Hubbard, E.J. Dick Jr., A.B. Cox, C. Schultz, Pallido-nigral spheroids in nonhuman primates: accumulation of heat shock proteins in astroglial processes, Acta Neuropathol. (Berl) 103 (2002) 276–280.

[40] J. Wu, N. Ichihara, D.H. Chui, K. Yamazaki, T. Kikuchi, Abnormal ubiquitination of dystrophic axons in centralnervous system of gracile axonal dystrophy (gad) mutant mouse, Alzheimer's Res. 47 (1996) 163–168.

[41] T. Yamada, H. Akiyama, P.L. McGeer, Two types of spheroid bodies in the nigral neurons in Parkinson's disease, Can. J. Neurol. Sci. 18 (1991) 287–294.

[42] K. Yamazaki, N. Wakasugi, T. Tomita, T. Kikuchi, M. Mukoyama, K. Ando, Gracile axonal dystrophy (GAD), a new neurological mutant in the mouse, Proc. Soc. Exp. Biol. Med. 187 (1988) 209–215.

[43] K. Yamazaki, H. Moriya, T. Wakabayashi, T. Kikuchi, Substance β-like immunoreactivity in the gracile nucleus and fasciculus in old mice, Neurosci. Lett. 106 (1989) 258–260.

[44] K. Yamazaki, A. Kobayashi, A. Kumazawa, T. Wakabayashi, K. Takeki, Axonal degeneration in the central nervous system of gracile axonal dystroph (gad) mice progresses like in human spinocerebellar ataxias, Biomed. Res. 12 (1991) 143–148.

Exp. Anim. 53(4), 391–394, 2004

—Note—

Comparative Study on Toxicokinetics of Bisphenol A in F344 Rats, Monkeys (Macaca fascicularis), and Chimpanzees (Pan troglodytes)

Takayuki NEGISHI[1,4], Toshikazu TOMINAGA[2], Yoshiyuki ISHII[1], Shigeru KYUWA[1], Ikuo HAYASAKA[2], Yoichiro KURODA[3,4], and Yasuhiro YOSHIKAWA[1,4]

[1]Department of Biomedical Science, Graduate School of Agricultural and Life Sciences, The University of Tokyo, 1–1–1 Yayoi, Bunkyo-ku, Tokyo 113-8657, [2]Kumamoto Primate Park, Sanwa Kagaku Kenkyusho, 990 Nishikuroiwa, Misumi, Kumamoto 869-3201, [3]Department of Molecular and Cellular Neurobiology, Tokyo Metropolitan Institute for Neuroscience, 2–6 Musashidai, Fuchu-shi, Tokyo 183-526, and [4]CREST, Japan Science and Technology Corporation, Kawaguchi-shi, Saitama 332-0012, Japan

Abstract: *We compared the toxicokinetics of bisphenol A (BPA) among three animal species: rats, cynomolgus monkeys and chimpanzees. Rats and monkeys were administered BPA orally or subcutaneously at 10 or 100 mg/kg body weight, while chimpanzees were administered only 10 mg/kg of BPA. BPA in serum was measured by ELISA. In oral administration of BPA at 10 mg/kg, both C_{max} and AUC were rats < chimpanzee < monkeys. In oral administration of BPA at 100 mg/kg, both C_{max} and AUC were rats < monkeys. Subcutaneous BPA administrations also revealed similar results, although the values of toxicokinetic parameters in subcutaneous administration were higher than those in oral administration. These results suggest that orally or subcutaneously administered BPA in primates is more easily absorbed than that in rats. We conclude that there are considerable differences in distribution, metabolism, and excretion of BPA between rodents and primates.*

Key words: *bisphenol A, chimpanzee, cynomolgus monkey*

Recently, there is an increasing concern about the risk of human exposure to bisphenol A (4,4'-isopropylidene-2-diphenol, BPA) which is a volume chemical used in the manufacture of polycarbonate plastics. BPA is known to have various hormone disrupting effects, such as estrogenic [4], anti-androgenic [14], and anti-thyroid activities [8]. Studies using rodents suggested that perinatal exposure to BPA results in abnormalities in reproductive function [16], hormonal function [11], central nervous system development [5, 12] and behavior [2, 9].

In toxicological studies, rodents, especially rats, are the most popular experimental animals. Considering human risk, however, primates would be more useful

(Received 24 December 2003 / Accepted 24 February 2004)

Address corresponding: T. Negishi, Department of Biomedical Science, Graduate School of Agricultural and Life Sciences, The University of Tokyo, 1–1–1 Yayoi, Bunkyo-ku, Tokyo 113-8657, Japan

because of their similarities to humans in their physiological characteristics. Chimpanzees, our closest relative, are considered to be the best models for humans among the non-human primates. Although there are a number of reports on the bioavailability of BPA in rats [6, 10, 15, 17] and monkeys [7], we tried for the first time to compare the toxicokinetics of BPA among three species, i.e., rats, cynomolgus monkeys and chimpanzees, to consider the human risk of BPA exposure. BPA was administered to animals of three species orally or subcutaneously at low (10 mg/kg) or high (100 mg/kg) doses to evaluate and compare dependency on dose as well as route of BPA administration among the three species.

Seventy-eight female F344/N rats (140–150 g body weight) were purchased from SLC (Shizuoka, Japan) and used for administrations of BPA. Collections of whole blood and serum preparations (see below) in rats were performed at the University of Tokyo (Tokyo, Japan). BPA administrations, collections of whole blood, and serum preparations in six female cynomolgus monkeys (*Macaca fascicularis*) (4.0 to 5.0 kg body weight), and the two female Western chimpanzees (*Pan troglodytes verus*) (40 to 50 kg body weight), were performed at Shin Nippon Biomedical Laboratory (Kagoshima, Japan) and Sanwa Kagaku Kenkyusho (Kumamoto, Japan), respectively. BPA (Tokyo Kasei Kogyo, Tokyo, Japan) was first dissolved in distilled water with 0.5% CM-cellulose (Wako Pure Chemical, Osaka, Japan) for oral administrations, and in a mixture of dimethylacetamide (Wako) and polyethylene glycol (Wako) (1 : 1) for subcutaneous administrations. BPA at 10 mg/kg or 100 mg/kg was administered to rats and monkeys by oral gavage or dorsal subcutaneous injection, while only 10 mg/kg BPA was administered to chimpanzees by the same ways as rats and monkeys for the ethical reason of avoiding any acute adverse effect at the higher dose of BPA (100 mg/kg). This study was approved by the Animal Care and Use Committee of the Graduate School of Agricultural and Life Sciences, the University of Tokyo. Rats were euthanatized by drawing whole blood under diethylether anesthesia before and 0.5, 1, 2, 4, 6, and 24 h after BPA administration (n=3 at each point). Monkeys (n=3 for 10 mg/kg and n=3 for 100 mg/kg) and chimpanzees (n=2 for 10 mg/kg) were first orally administered BPA at the two dosages and low dose (10 mg/kg), respectively. After one week for entire excretion of BPA [3], the above dosages were repeated subcutaneously. Serial blood samples were taken from each monkey before and 0.5, 1, 2, 4, 6, and 24 h after administration or from each chimpanzee before and 0.25, 0.5, 1, 2, 3, 4, 8, and 24 h after administration. Serum samples were harvested by centrifugation at 3,000 g for 15 min and were kept at –20°C until analysis. BPA in serum was measured by BPA ELISA kit (Japan EnviroChemicals, Japan). Methanol was first added to the serum (1:5, methanol: serum), and then the sample was centrifuged at 10,000 g for 15 min. Supernatant was diluted with the same volume of purified water. Prepared samples were subjected to ELISA according to product manuals. Briefly, the sample and the antigen (BPA)-enzyme complex solution were mixed and added to each microplate well, the inside of which was coated with the BPA-specific antibody. After 60 min competitive assay, unbound or excess reagents were washed out and substrate chromogen was added to each well to develop the color. The optical density at 490 nm was measured to determine the amount of BPA in the sample. In the present method, the detection limit of BPA in serum was 12.5 μg/L. Toxicokinetic parameters were determined from the individual serum BPA concentration-time curves. Peak serum concentrations (C_{max}) and the time to reach C_{max} (T_{max}) were obtained from observed data. The area under the serum BPA concentration-time curves for 4 h ($AUC_{0-4\,h}$) and for 24 h ($AUC_{0-24\,h}$) were calculated by the linear trapezoidal method.

The concentration-time profiles of oral BPA administration at 10 mg/kg in rats, monkeys and chimpanzees, and those at 100 mg/kg in rats and monkeys are shown in Figs. 1A and B, respectively. These profiles indicate lower BPA bioavailability in rats compared to that in both monkeys and chimpanzees. Indeed, no sample of rats contained detectable levels of BPA except for one (33 μg/L) of three samples at 2 h after oral BPA administration at 10 mg/kg, thus C_{max}, $AUC_{0-4\,h}$, and $AUC_{0-24\,h}$ could not be calculated (Table 1), and T_{max} was not defined. In oral administration of BPA at 10 mg/kg, C_{max}, $AUC_{0-4\,h}$, and $AUC_{0-24\,h}$ showed the same tendency, that is, rats < chimpanzees < monkeys (Table 1). In oral administration of BPA at 100 mg/kg, C_{max}, $AUC_{0-4\,h}$, and $AUC_{0-24\,h}$ were all rats < monkeys (Table 1). Subcutaneous BPA administrations at 10 or 100

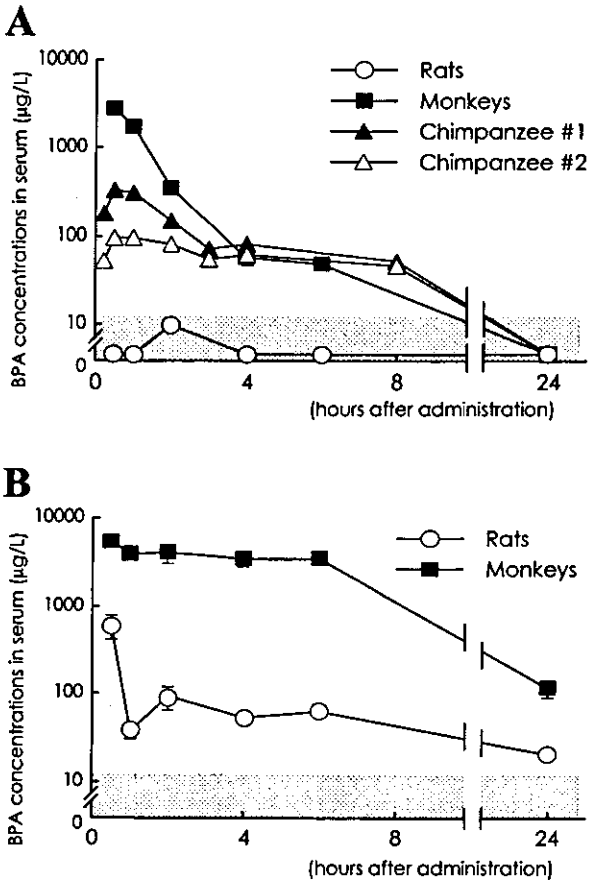

Fig. 1. Serum levels of bisphenol A after oral administration at 10 mg/kg in female rats, monkeys and chimpanzees (A), and at 100 mg/kg in rats and monkeys (B). Data represent the mean ± SEM of three rats and three monkeys. Data of chimpanzees are indicated as plots from each subject (chimpanzee #1 and #2). No error bar in rats or monkeys indicates that the error is included within the symbol. Plots in gray area mean that serum BPA concentration is under the detection limit in this study.

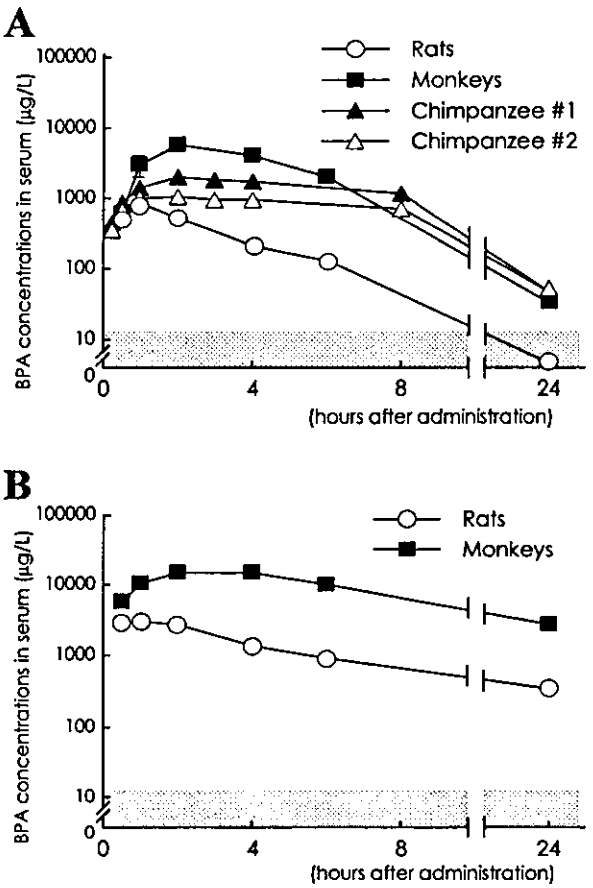

Fig. 2. Serum levels of bisphenol A after subcutaneous administration at 10 mg/kg in female rats, monkeys and chimpanzees (A), and at 100 mg/kg in rats and monkeys (B). Data represent the mean ± SEM of three rats and three monkeys. See also the figure legend of Fig. 1.

mg/kg showed similar results, although the values of toxicokinetic parameters were higher than those in oral administrations at each dose (Fig. 2 and Table 1).

We demonstrated the direct comparison of toxicokinetics of oral or subcutaneous administration of BPA among F344 rats, cynomolgus monkeys, and Western chimpanzees. Oral administration resulted in lower availability of BPA when compared to subcutaneous administration in all species examined in this study, suggesting a route dependency common to mammals, which is consistent with a previous report [10]. Fast-pass metabolism by the intestine and/or liver as well as intestinal secretion probably contributed to the lower bioavailability of orally administered BPA. We also observed clear dose dependency in toxicokinetic parameters between 10 and 100 mg/kg administrations in rats and monkeys as expected. Irrespective of route of administration, bioavailabilities of BPA at 10 or 100 mg/kg were rats < chimpanzees < monkeys, or rats < monkeys, respectively, in this study. These results suggest that either orally or subcutaneously administered BPA in primates is more easily absorbed than in rats. This might be due to the differences in the abilities of metabolism and/or excretion of BPA between rats and monkeys. Further researches about the species differences in alteration of hepatic and intestinal enzyme expression and function accompanying BPA disposi-

Table 1. Toxicokinetic parameters in rats, monkeys, and chimpanzees after oral or subcutaneous injection of BPA at 10 or 100 mg/kg

	10 mg/kg BPA			100 mg/kg BPA	
	Rats (n=3)[a] (mean±SD)	Monkeys (n=3) (mean±SD)	Chimpanzees (#1, #2)	Rats (n=3) (mean±SD)	Monkeys (n=3) (mean±SD)
Oral injection					
C_{max} (μg/L)	N.C.[b]	2,793 ± 920	325, 96	580 ± 398	5,732 ± 525
T_{max} (h)	N.D.[c]	0.7 ± 0.2	0.5, 0.5	0.5	0.7 ± 0.2
$AUC_{0-4\,h}$ (μg·L^{-1}·h)	N.C.	3,209 ± 536	491, 235	506 ± 313	14,747 ± 2,495
$AUC_{0-24\,h}$ (μg·L^{-1}·h)	N.C.	3,247 ± 587	1,167, 813	1,353 ± 462	52,595 ± 8,951
Subcutaneous injection					
C_{max} (μg/L)	872 ± 164	57,934 ± 1,902	2,058, 1,026	3,439 ± 679	10,851 ± 3,915
T_{max} (h)	1.0	2.0 ± 0.0	2.0, 2.0	1.0	2.0 ± 0.0
$AUC_{0-4\,h}$ (μg·L^{-1}·h)	1,912 ± 262	15,316 ± 5,856	5,658, 3,109	9,314 ± 2,634	48,010 ± 11,641
$AUC_{0-24\,h}$ (μg·L^{-1}·h)	3,377 ± 334	39,040 ± 10,738	21,141, 12,492	23,001 ± 6,387	189,627 ± 21,790

[a] Note that T_{max}, in rats was determined by using the mean of each time point. C_{max} in rats represents mean ± SD calculated by the serum BPA concentrations of three animals at T_{max}. [b] N.C.: Not calculated. [c] N.D.: Not defined.

tion, such as CYP450 and UDP-glucuronosyl transferase (UDPGT), among rodents and primates are important, since BPA is metabolized principally to its monoglucuronide conjugate and is excreted via feces or urine [13]. It is possible that humans might also absorb BPA more easily than experimental rats. Both behavioral and neurological alterations in rodents by perinatal low-dose BPA exposure per os even at < 100 μg/kg/day [1] would strongly suggest potential adverse effects of chronic environmental exposure to BPA in humans (< 10 μg/kg/day), if the differences in bioavailability between rodents and primates including humans also applies to much lower dose exposure to BPA. We conclude that there are considerable differences in distribution, metabolism, and excretion of BPA between rodents and primates.

References

1. Adriani, W., Seta, D.D., Dess-Fulgheri, F., Farabollini, F., and Laviola, G. 2003. *Environ. Health Perspect.* 111: 395–401.
2. Farabollini, F., Porrini, S., and Dessi-Fulgherit, F. 1999. *Pharmacol. Biochem. Behav.* 64: 687–694.
3. Knaak, J.B. and Sullivan, L.J. 1966. *Toxicol. Appl. Pharmacol.* 8: 175–184.
4. Krishnan, A.V., Stathis, P., Permuth, S.F., Tokes, L., and Feldman, D. 1993. *Endocrinology* 132: 2279–2286.
5. Kubo, K., Arai, O., Ogata, R., Omura, M., Hori, T., and Aou, S. 2001. *Neurosci. Lett.* 304: 73–76.
6. Kurebayashi, H., Betsui, H., and Ohno, Y. 2003. *Toxicol. Sci.* 73: 17–25.
7. Kurebayashi, H., Harada, R., Stewart, R.K., Numata, H., and Ohno, Y. 2002. *Toxicol. Sci.* 68: 32–42.
8. Moriyama, K., Tagami, T., Akamizu, T., Usui, T., Saijo, M., Kanamoto, N., Hataya, Y., Shimatsu, A., Kuzuya, H., and Nakao, K. 2002. *J. Clin. Endocrinol. Metab.* 87: 5185–5190.
9. Negishi, T., Kawasaki, K., Takatori, A., Ishii, Y., Kyuwa, S., Kuroda, Y., and Yoshikawa, Y. 2003. *Environ. Toxicol. Pharmacol.* 14: 99–108.
10. Pottenger, L.H., Domoradzki, J.Y., Markham, D.A., Hansen, S.C., Cagen, S.Z., and Waechter Jr, J.M. 2000. *Toxicol. Sci.* 54: 3–18.
11. Rubin, B.S., Murray, M.K., Damassa, D.A., King, J.C., and Soto, A.M. 2001. *Environ. Health Perspect.* 109: 675–680.
12. Sato, K., Matsuki, N., Ohno, Y., and Nakazawa, K. 2002. *Neuroendocrinology* 76: 223–234.
13. Snyder, R.W., Maness, S.C., Gaido, K.W., Welsch, F., Sumner, S.C., and Fennell, T.R. 2000. *Toxicol. Appl. Pharmacol.* 168: 225–234.
14. Sohoni, P. and Sumpter, J.P. 1998. *J. Endocrinol.* 158: 327–339.
15. Upmeier, A., Degen, G.H., Diel, P., Michna, H., and Bolt, H.M. 2000. *Arch. Toxicol.* 74: 431–436.
16. vom Saal, F.S., Cooke, P.S., Buchanan, D.L., Palanza, P., Thayer, K.A., Nagel, S.C., Parmigiani, S., and Welshons, W.V. 1998. *Toxicol. Ind. Health* 14: 239–260.
17. Yoo, S.D., Shin, B.S., Lee, B.M., Lee, K.C., Han, S.Y., Kim, H.S., Kwack, S.J., and Park, K.L. 2001. *J. Toxicol. Environ. Health. A* 64: 417–426.

Available online at www.sciencedirect.com
SCIENCE DIRECT®
Neuroscience Research 49 (2004) 339–346
Neuroscience Research
www.elsevier.com/locate/neures

Astroglial responses against Aβ initially occur in cerebral primary cortical cultures: species differences between rat and cynomolgus monkey

Nobuyuki Kimura*, Takayuki Negishi, Yoshiyuki Ishii, Shigeru Kyuwa, Yasuhiro Yoshikawa

Department of Biomedical Science, Graduate School of Agricultural and Life Sciences, the University of Tokyo, 1-1-1 Yayoi, Bunkyo-ku, Tokyo 113-8657, Japan

Received 5 February 2004; accepted 29 March 2004

Available online 6 May 2004

Abstract

In the present study, we investigated how amyloid beta (Aβ) peptides initially affect neuronal cells in primary cerebral cortical cultures from rat and cynomolgus monkey. In these cultures, complicated interactions between glial and neuronal cells occur; moreover, synaptic interactions similar to those observed in vivo also occur between neuronal cells in these cultures. In this study, we applied low concentrations of Aβ to these well-characterized primary cultures to investigate how Aβ initially affects neurons or astroglial cells. In both rat and monkey cortical cultures, treatment with low concentrations of Aβ failed to drastically change or damage of neurons. Aβ treatment, however, significantly activated astrocytes, resulting in increased apolipoprotein E (ApoE) production. Rat astrocytes were more sensitive to Aβ than monkey astrocytes, and responded to Aβ via a different mechanism. In monkey astrocyte cultures, only direct treatment with Aβ increased ApoE production. In rat astrocyte cultures, however, treatment with conditioned media from cortical cultures grown with Aβ increased ApoE production, indicating that some sort of neuron-derived soluble factor(s) was also involved in activating rat astrocytes. These species differences suggest that monkey cortical cultures would be more useful as an in vitro model system to understand the details of how Aβ accumulates in the human brain, since monkeys are phylogenetically more similar to humans.

Keywords: Amyloid beta peptides; Astrocyte; Monkey cortical culture; Rat cortical culture; Species difference

1. Introduction

Amyloid beta (Aβ) peptide consists of 40–43 amino acids and is derived from amyloid precursor protein (APP) (Citron et al., 1997). Aβ is the major protein component of senile plaques (SP), a characteristic feature of Alzheimer's disease (AD) (Glenner, 1988). Since Aβ is toxic to cultured nerve cells, some have argued that Aβ cytotoxicity is the major cause of brain damage observed in AD (Behl et al., 1992; Koh et al., 1990; Mattson et al., 1992; Yankner et al., 1990). Although Aβ toxicity has been thoroughly studied, the manner in which neuronal cells in vivo are initially affected by Aβ accumulation remains unknown.

Many studies also show that astrocytes have an important role in clearing Aβ from the brain (Funato et al., 1998; Matsunaga et al., 2003; Wyss-Coray et al., 2003). We previously showed that both neuronal and glial cells are found in primary cultures prepared from the cerebral cortices of either rat or cynomolgus monkeys (Negishi et al., 2002a,b). In these cultures, complicated interactions between glial and neuronal cells occur; moreover, synaptic interactions similar to those observed in vivo also occur between neuronal cells in these cultures. In the present study, we applied low concentrations of Aβ to these well-characterized primary cultures to investigate how Aβ initially affects neurons or astroglial cells. Since SP are conformed by the aggregation of low concentrations of Aβ with age, Aβ treatment in this study would reflects in vivo event of the early stage of Aβ accumulation. We also investigated how astroglial cells respond to Aβ when conditioned media are applied to the cultures. We were especially interested in determining whether species (rat versus monkey) differences emerged in the responses of neuronal and astroglial cells to Aβ.

* Corresponding author. Tel.: +81-3-5841-5037; fax: +81-3-5841-8186.
E-mail address: aa07190@mail.ecc.u-tokyo.ac.jpco (N. Kimura).

0168-0102/$ – see front matter © 2004 Elsevier Ireland Ltd and The Japan Neuroscience Society. All rights reserved.
doi:10.1016/j.neures.2004.03.010

2. Materials and methods

2.1. Animals

Pregnant Sprague-Dawley rats were purchased from SLC Japan (Shizuoka, Japan). The animals were maintained under controlled conditions (temperature, 24 ± 1 °C; humidity,55 ± 5%) in plastic cages with sterilized wood shavings for bedding. They were fed a commercially available diet (CMF; Oriental Yeast, Tokyo, Japan) and had ad libitum access to food and tap water.

Six cynomolgus monkey (*Macaca fascicularis*) fetuses (80 days gestation) were used in this study. Four were purchased from Shin Nippon Biomedical Laboratories (Kagoshima, Japan), and two were obtained from the Tsukuba Primate Center, National Institute of Infectious Diseases, Japan. This experiment was conducted according to the guidelines of the Animal Care and Use Committee of the Graduate School of Agricultural and Life Sciences, The University of Tokyo.

2.2. Rat primary cerebral cortical cultures

Rat fetuses were removed on gestational day 18 by axillary exsanguination, and their brains were removed then transferred into ice-cold isolation medium (IM) consisting of equal volumes of Ca^{2+}-free phosphate-buffered saline (PBS), Mg^{2+}-free PBS, and Dulbecco's Modified Eagle's Medium containing 1.2 mg/ml $NaHCO_3$, 110 μg/ml pyruvic acid, 25 μg/ml streptomycin, and 50 U/ml penicillin (mDMEM). After bisecting the brains into cerebral hemispheres, the meninges, hippocampi, and other subcortical structures were carefully removed, and the cerebral cortices were rinsed in culture medium (CM: mDMEM with 5% fetal calf serum) and minced into small pieces (<1 mm^3) in CM. The tissue pieces were digested at 32 °C for 30 min in PBS containing 1.5 U/ml papain (Worthington Biochemical Corporation, Lakewood, NJ, USA), 0.1 mg/ml DNase I (Roche Diagnostics, Japan), 0.2 mg/ml cysteine, 0.2 mg/ml albumin, and 5 mg/ml glucose. Cells were dissociated gently by passing the mixture several times through a disposable pipette, and then the mixture was centrifuged three times in CM at 800 rpm for 5 min at 32 °C. For TUNEL staining, cells were plated at 2.5×10^5 cells/cm^2 in CM onto a LAB-TEK chamber slide (Nalge Nunc, Tokyo, Japan) coated with 0.125% polyethylenimine. For other experiments, cells were plated at 4.2×10^5 cells/cm^2 onto culture dishes coated with 0.125% polyethylenimine. All cultures were maintained at 37 °C in a humidified chamber containing 95% air and 5% CO_2. Half the volume of culture supernatant was replaced with pre-warmed CM once per week.

These primary rat cerebral cortical cultures consist mainly of neurons (more than 90%) with some astrocytes. We previously showed that these cultured neuronal cells have complicated interactions with glia and other neurons and make synaptic connections with other neurons similar to those in vivo (Negishi et al., 2002a). After 3 days in vitro, the total proteins of these cultures almost unchanged regardless of time course (data not shown).

2.3. Cynomolgus monkey primary cerebral cortical cultures

Monkey fetuses were removed on gestational day 80, and then digested and dissociated in the identical manner as for the rat cultures (above). Plating onto slides and culture dishes for TUNEL staining and other experiments was carried out in exactly the same way as for the rat cultures. As with the rat cultures, half the volume of culture supernatant was replaced with pre-warmed CM once per week.

As with the rat cultures, these monkey primary cerebral cortical cultures consisted mainly of neurons (more than 90%) with some astrocytes. We previously showed that these cultures also exhibit complicated interactions similar to those observed under in vivo conditions (Negishi et al., 2002b). After 3 days in vitro, the total proteins of these cultures almost unchanged regardless of time course such as rat (data not shown).

2.4. Rat and cynomolgus monkey astrocyte cultures

After 14 days of culturing, cerebral cortical cells were dissociated with 0.025% trypsin (Invitrogen, UK) and washed several times in CM. Proliferating type-1 astrocytes were quickly selected from this suspension. After one subculturing, cells were plated at 4.2×10^5 cells/cm^2 in CM onto uncoated culture dishes. Half the volume of culture supernatant was replaced with pre-warmed CM once per week (Negishi et al., 2003).

2.5. Amyloid beta treatment

Aβ peptides, Aβ1-40 (Aβ40) and Aβ1-42 (Aβ42) (Bachem, Torrance, CA, USA), were dissolved in 100% DMSO, then diluted in CM (0.45% DMSO final concentration). These Aβ40 and Aβ42 (i.e., no pre-aggregating) were ultimately added to primary cortical cultures and astrocyte cultures. After 3 days of culturing, CM containing Aβ peptides was added into the rat or monkey cortical primary cultures at a concentration of 2 μM or 5 μM. These cultures were maintained for 1, 3, 7, or 14 days. Aβ peptides (5 μM) were also added to confluent rat or monkey astrocyte cultures, and these were maintained for 3 days. The CM of control cultures contained the same concentration of DMSO (0.45%).

2.6. Treatment with conditioned media

To examine whether soluble factors produced by neurons affect astrocyte responses to Aβ peptides, the conditioned medium from the primary cortical cultures was collected and used to treat the astrocyte cultures. CM supernatant from the rat and monkey primary cultures was collected after 1, 3,

and 7 days of Aβ treatment (5 μM). Astrocyte cultures (see above) from rat or monkey were maintained in the respective supernatant for 3 days.

2.7. Antibodies

For Western blotting, the following antibodies were used: rabbit polyclonal anti-Caspase-3 (H277; Santa Cruz Biotechnology, Santa Cruz, CA, USA), mouse monoclonal anti-Synaptophysin (SY38; DAKO, Denmark), rabbit polyclonal anti-APP (β-APP_{695}; Zymed Laboratories, San Francisco, CA, USA), mouse monoclonal anti-GSK3β (GSK; Transduction Laboratories, Lexington, KY, USA), rabbit polyclonal anti-phospho-GSK3β (S9; Cell Signaling Technology, Beverly, MA, USA), mouse monoclonal anti-Glial fibrillary acidic protein (6F2; DAKO, Denmark), and goat polyclonal anti-ApoE (APO-E; Chemicon). H277 reacts not only with p11, p17, and p20 subunits but also with the full-length precursor of caspase-3. β-APP_{695} reacts with all three forms of β-APP (β-APP_{695}, β-APP_{751}, β-APP_{770}) and recognizes the APP C-terminal fragment (βCTF) that results from the cleavage of APP by β-secretase. S9 recognizes the Ser-9-phosphorylated, inactive form of GSK3β.

2.8. Western blot analyses

To extract total cellular proteins from the cultured cells, the cells were bathed in a solution containing 9.85 mg/ml Tris–HCl, 0.774 mg/ml ethylenediaminetetraacetic acid (EDTA), 0.348 mg/ml ammonium persulfate, 0.5% (v/v) TritonX-100, and 2.3% (w/v) SDS in PBS. Total proteins were isolated by centrifugation, adjusted to 30 μg, then subjected to SDS-polyacrylamide gel electrophoresis (SDS-PAGE with 12.5% acrylamide gel). Separated proteins were blotted onto polyvinylidene fluoride membranes (Immobilon P, Millipore, Bedford, MA, USA). The membranes were blocked with 5% nonfat dried milk in 20 mM PBS (pH 7.0) and 0.1% Tween-20 overnight at 4 °C, then incubated with primary antibodies (H277, 1:2000; Syn, 1:5000; β-APP_{695}, 1:2000; GSK, 1:10,000; S9, 1:1000; GFAP, 1:10,000; APO-E, 1:3000) for 1 h at room temperature. They were then incubated with horseradish peroxidase-conjugated goat anti-mouse IgG, mouse anti-rabbit IgG, or rabbit anti-goat IgG (1:6000, Jackson Immunoresearch Laboratories, West Grove, PA, USA) for 1 h at room temperature. Immunoreactive elements were visualized using enhanced chemiluminescence (ECLplus, Amersham, UK).

2.9. Data analyses

The effects of Aβ treatment on the expression of synaptophysin, APP-βCTF, GSK3β, capsase-3, GFAP, and ApoE were confirmed by quantifying the immunoreactive bands (obtained from the Western blots) with commercially available software (Quantity One, PDI, Inc, NY, USA). Data are shown as means ± S.D. For statistical analyses, one-way ANOVAs were performed followed by the Bonferroni/Dunn *post hoc* test.

3. Results

3.1. Western blot analyses of neuron- and astrocyte-related protein expression following aβ treatment

Western blot analyses were performed to determine whether Aβ treatment affected the expression of various neuron- and glia-related proteins. In rat cortical cultures, treatment with either Aβ40 or Aβ42, even at a concentration of 5 μM, did not significantly influence the expression of synaptophysin, APP-βCTF, or GSK3β (Figs. 1A and 2A–C). Aβ40 and Aβ42 also did not affect the expression of the full-length precursor of caspase-3 in these cells; moreover, expression of all caspase-3 subunits was absent, regardless of the duration of Aβ treatment (data not shown). Synaptophysin expression did not decrease even after 14 days of Aβ treatment; rather, synaptophysin expression

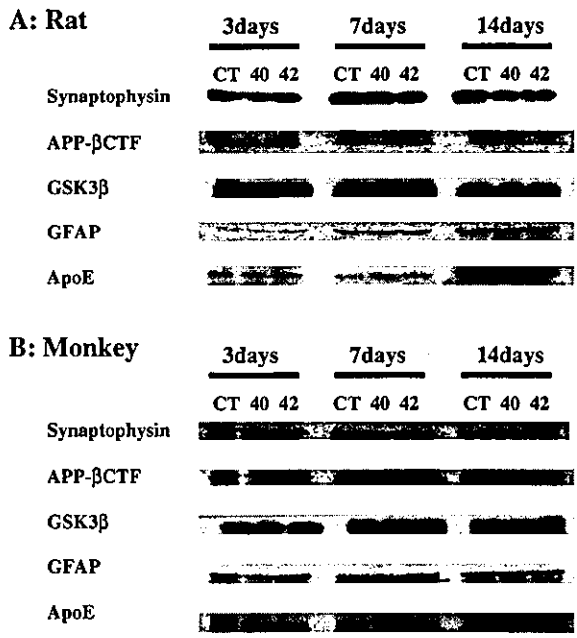

Fig. 1. Western blots showing the expression of neuron-related proteins (synaptophysin, APP-βCTF, and GSK3β) and astrocyte-related proteins (GFAP and ApoE) in rat primary cerebral cortical cultures (A) and monkey primary cerebral cortical cultures (B) following treatment with either 5 μM Aβ40 or 5 μM Aβ42. SY38 immunostained a 38 kDa band representing synaptophysin, β-APP_{695} immunostained a ~15 kDa band representing APP-βCTF, and GSK immunostained a 46 kDa band representing GSK3β. 6F2 immunostained a 52 kDa band representing GFAP, and APO-E immunostained a ~34 kDa band representing ApoE. CT—controls consisted of extracts from cultures grown in standard culture medium with DMSO; 40—extracts from cultures treated with Aβ40; 42—extracts from cultures treated with Aβ42; 3 days—after 3 days of Aβ treatment; 7 days—after 7 days of Aβ treatment; 14 days—after 14 days of Aβ treatment.

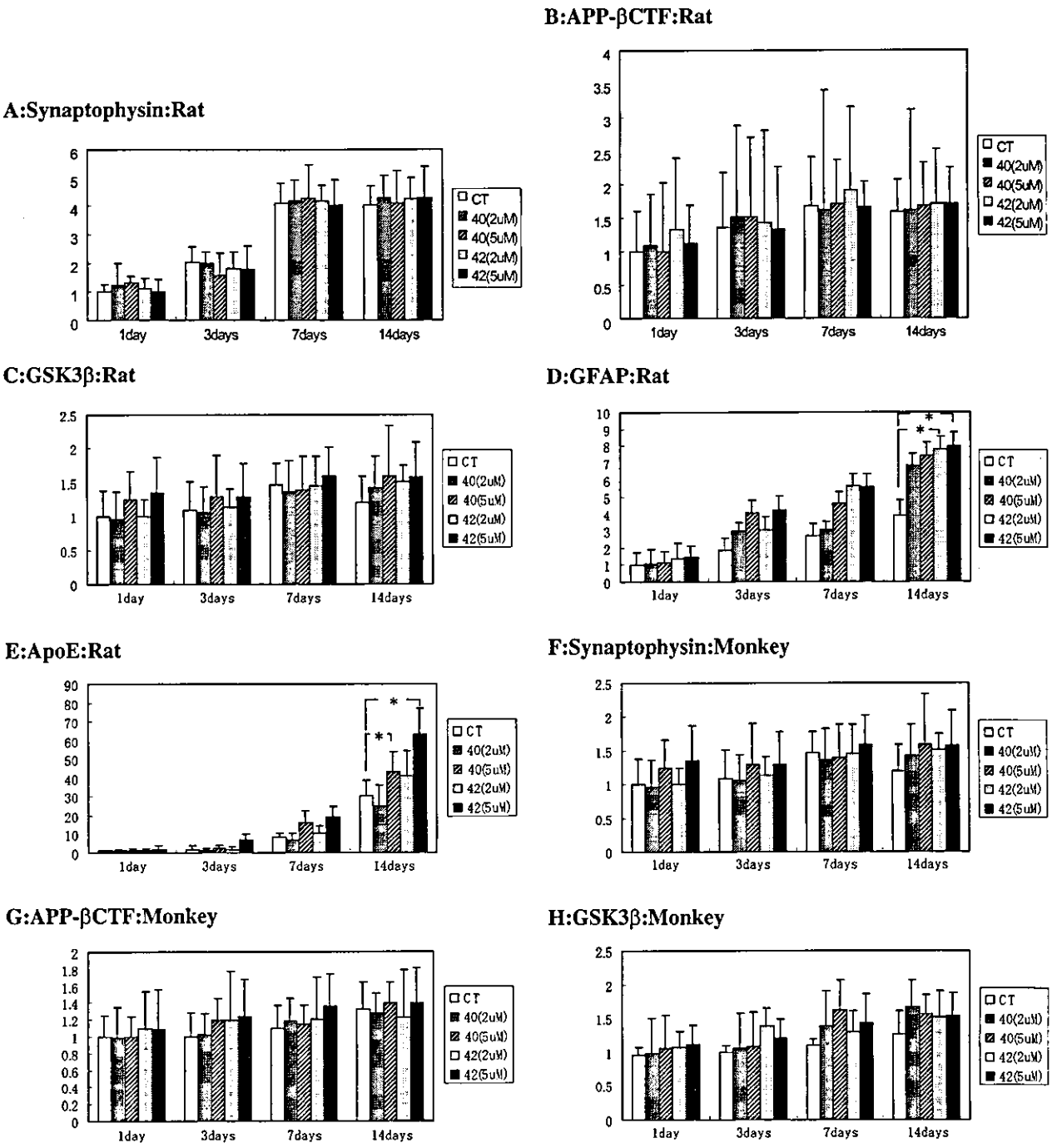

Fig. 2. Immunoreactive bands were quantified, and the resulting density data were compared to those measured from blots containing extracts from control cultures grown for 1 day (*$P < 0.02$). In rat cortical cultures ($N = 10$) (A–E): Aβ treatment did not significantly affect the expression of synaptophysin (A), APP-βCTF (B), and GSK3β (C). Interestingly, synaptophysin expression measured 7 and 14 days after Aβ treatment was slightly elevated and greater than that measured after 1 and 3 day(s) of Aβ treatment. In contrast to the neuron-related proteins, Aβ treatment induced increases in expression of astrocyte-related proteins. GFAP expression was significantly elevated in cultures treated with either 2 μM or 5 μM Aβ42 for 14 days (D). ApoE expression was significantly elevated in cultures treated with either 5 μM Aβ40 or 5 μM Aβ42 treatments (E). In monkey cortical cultures ($N = 6$) (F–J), Aβ treatment did not affect the expression of synaptophysin (F), APP-βCTF (G), and GSK3β (H). Although GFAP levels did not markedly increase in cultures treated with Aβ, even after 14 days of Aβ treatment (I), ApoE expression significantly increased in cultures treated with 5 μM Aβ42 for 14 days (J). Data are means and error bars are S.D.s.

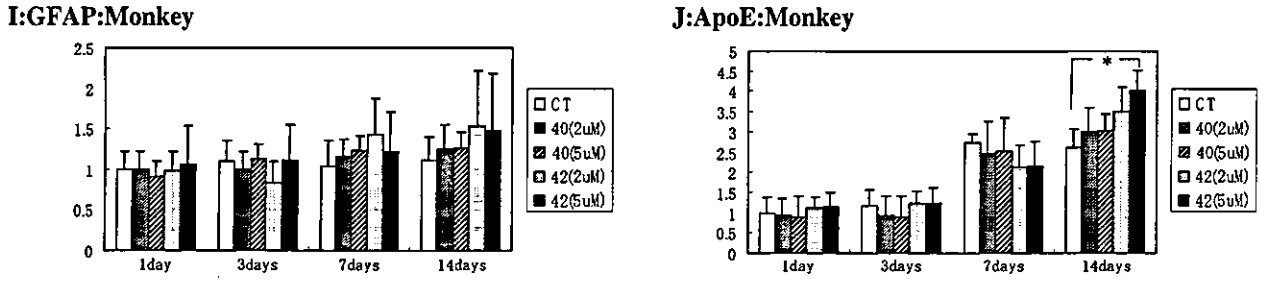

Fig. 2. (*Continued*).

was greater 14 days after treatment compared to that 3 days after treatment (Fig. 2A). APP-βCTF expression remained unchanged throughout the course of Aβ treatment, even after 14 days, indicating that Aβ treatment did not induce endogenous Aβ production from APP (Figs. 1A and 2B). GSK3β expression slightly increased in cultures treated with Aβ (Figs. 1A and 2C). However, levels of Ser-9-phosphorylated GSK3β, the inactive form of GSK3β, remained unchanged regardless of Aβ treatment length or concentration of Aβ (data not shown). Similarly, the expression of neuron-related proteins in monkey cortical cultures did not significantly decrease or increase during Aβ treatment (Figs. 1B and 2F–H).

In stark contrast to neuron-related proteins, we found that Aβ treatment profoundly affected astrocyte-related proteins in both rat and monkey cortical cultures (Figs. 1 and 2D,E,I,J), and the effects were different for the two species.

In rat cortical cultures, 14 days of Aβ42 treatment, even at a low concentration of 2 μM, increased GFAP expression significantly (Figs. 1A and 2D). Aβ40 treatment also increased GFAP expression, but not significantly (Fig. 2D). In addition, both Aβ40 and Aβ42 treatment (5 μM) significantly increased ApoE expression (Figs. 1A and 2E). On the other hand, in monkey cortical cultures, 14 days of Aβ42 treatment only slightly increased GFAP expression (Figs. 1B and 2I). Furthermore, only Aβ42 treatment (5 μM for 14 days) significantly increased ApoE expression; the magnitude of this increase was less than that observed in correspondingly treated rat cortical cultures (Fig. 2E,J).

3.2. Western blot analyses of astrocyte-related protein expression following treatment with conditioned media

To examine whether some kind of neuron-derived soluble factor(s) influences astrocytic responses to the different Aβ peptides in cortical cultures, we treated rat and monkey astrocyte cultures with either conditioned media from primary cultures treated with Aβ or media containing Aβ (i.e., direct Aβ treatment), then we compared the changes in the expression levels of astrocyte-related proteins (GFAP and ApoE). In rat astrocyte cultures, direct Aβ42 treatment significantly increased GFAP expression (Figs. 3A and 4A). On the other hand, conditioned-media treatment did not affect GFAP expression in astrocyte cultures, even when the conditioned medium was derived from cortical cultures treated with Aβ for 7 days (Figs. 3A and 4A). In monkey astrocyte cultures, direct Aβ treatment also increased GFAP expression, although not significantly (Figs. 3B and 4C). Similar to rat astrocyte cultures, conditioned-media treatment did not affect GFAP expression in monkey astrocyte cultures. Although direct Aβ treatment induced expression of GFAP and conditioned-media treatment had little effect in both rat and monkey astrocyte cultures, the opposite occurred for ApoE (Figs. 3 and 4B,D). In rat astrocyte cultures, direct Aβ treatment induced ApoE expression, and furthermore, treatment with conditioned medium from cortical cultures treated with Aβ42 for either 3 or 7 days also increased ApoE expression levels significantly (Figs. 3A and 4B). Treatment with conditioned media from cortical cultures treated with Aβ40 also induced ApoE expression, but not significantly (Fig. 4B). The degree of ApoE increase depended on the source of the conditioned medium (i.e., media collected from cortical cultures treated with Aβ for 1, 3, or 7 days) (Fig. 4B). In contrast to rat astrocyte cultures, in monkey astrocyte cultures, only direct treatment with Aβ42 significantly increased ApoE expression levels (Figs. 3B and 4D). Direct Aβ40 treatment, as well as any

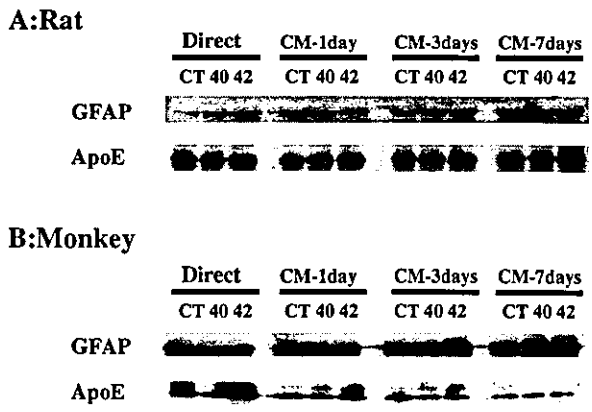

Fig. 3. Western blots showing the expression of GFAP and ApoE in extracts from rat astrocyte cultures (A) and monkey astrocyte cultures (B) following direct treatment with Aβ or treatment with conditioned media from cortical cultures treated with Aβ for 3 days. Direct—direct Aβ treatment; CM—treatment of astrocyte cultures with conditioned medium collected from cortical cultures exposed to Aβ for 1, 3 or 7 days; CT—control; 40—Aβ40 treatment; 42—Aβ42 treatment.

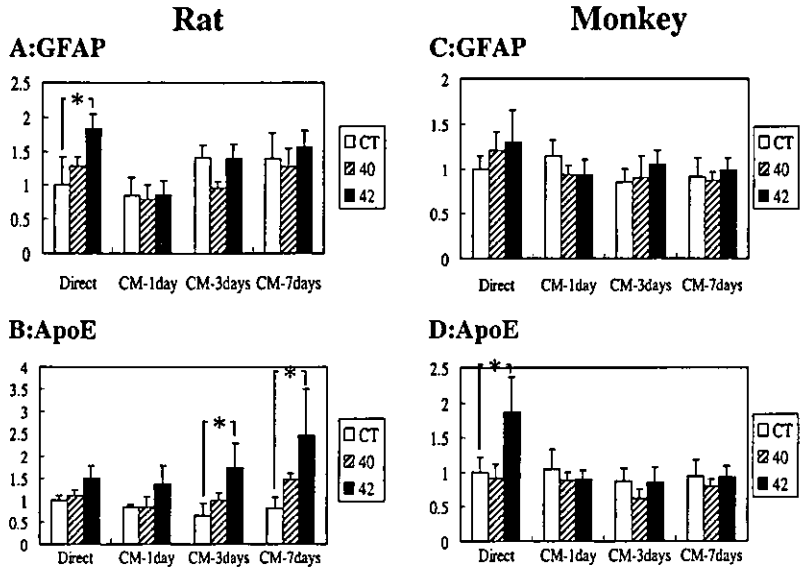

Fig. 4. Immunoreactive bands shown in Fig. 3 were quantified, and the resulting density data were compared to those measured from blots containing extracts from control cultures ($*P < 0.02$). In rat astrocyte cultures ($N = 6$) (A, B), direct treatment with Aβ42 significantly increased GFAP expression levels (A). Direct treatment with Aβ42 increased ApoE expression levels, and furthermore, treatment with conditioned media from cortical cultures treated with Aβ42 for either 3 or 7 days significantly increased ApoE expression (B). The degree of ApoE increase was directly correlated with the number of days the cortical cultures were treated with Aβ. In monkey astrocyte cultures ($N = 6$) (C, D), direct treatment with Aβ42 slightly increased GFAP expression (C). Direct treatment with Aβ42 significantly increased ApoE expression (D). Labeling conventions as in Fig. 3.

of the conditioned-media treatments (i.e., Aβ40, Aβ42, or duration of Aβ exposure), failed to affect ApoE expression levels in monkey astrocyte cultures (Fig. 4D).

4. Discussion

Aβ was previously shown to induce neuronal apoptosis, activate GSK3β, and lead to the accumulation of newly synthesized intracellular Aβ in APP-transfected cells (Cardoso et al., 2002; Ivins et al., 1999; Loo et al., 1993; Mattson et al., 1998; Morishima et al., 2001; Troy et al., 2000; Takashima et al., 1998; Yang et al., 1999). Although these studies shed much light on the various phenomena induced by Aβ, the initial effects of or disturbances caused by Aβ accumulation in the brain remain unknown; astroglial responses primarily occur, or neuronal injuries primarily happen. In the brain, small quantities of Aβ typically accumulate with age; and in some cases, this accumulated Aβ aggregates, causing Aβ-associated pathologies such as AD (Selkoe, 1991). In the present study, we sought to clarify events that may occur early on during the initial stages of Aβ accumulation and aggregation. This was achieved by assessing cultured neuronal cells for signs of apoptosis and altered expression of certain proteins following long-term treatment (14 days) with relatively low concentrations of "no pre-aggregating" forms of Aβ.

In both rat and monkey cortical cultures, Aβ did not significantly decrease or increase expression of caspase-3 or the neuron-related proteins synaptophysin, APP-βCTF, and GSK3β (Figs. 1, 2A–C,F–H, data not shown for caspase-3). These results indicate that Aβ had no effect on neurons during the initial stages of Aβ accumulation and aggregation, indicating that Aβ and its subsequent accumulation and aggregation did not appear to disrupt the formation of synapses.

On the other hand, Aβ treatment increased the expression of the astrocyte-related proteins GFAP and ApoE in both rat and monkey cortical cultures (Fig. 1D,E,I,J), indicating that astroglia, rather than neurons, may be the first neural cells affected by the initial accumulation and aggregation of Aβ in the brain. During the initial stages of Aβ accumulation, therefore, one would intuitively expect to detect astroglial responses (e.g., changes in the expression of astroglia-related proteins) before neuronal responses (e.g., neuronal injury or apoptosis).

The astroglial responses to Aβ differed somewhat in rat and monkey cortical cultures, suggesting possible species differences in how astrocytes react to the accumulation and aggregation of Aβ. In rat cortical cultures, Aβ treatment tended to increase GFAP and ApoE expression levels to a greater degree than in monkey cortical cultures (Figs. 1 and 2D,E,I,J). This finding suggests that rat neuronal cells may be more sensitive to Aβ (thus requiring a greater astroglial response), whereas monkey neuronal cells may be more resistant to Aβ (thus requiring a lesser astroglial response). Cynomolgus monkeys are old world monkeys classified as nonhuman primates and are more similar to humans than rats. Extrapolation of these results, therefore, to humans leads to the prediction that neurons in the human brain may be more resilient than previously thought and may resist

damage during the early stages of Aβ accumulation, thereby allowing astrocytes more time to react and remove excess Aβ from the brain before neuronal injury can occur.

The astroglial responses to different forms of Aβ also differed. In both rat and monkey cortical cultures, Aβ42 treatment increased GFAP and ApoE levels to a greater extent than in cultures receiving Aβ40 treatment (Figs. 1 and 2). Several studies have shown that Aβ42 is more closely associated with AD pathogenesis than Aβ40 (Burdick et al., 1992; Jarrett et al., 1993; Suzuki et al., 1994; Younkin, 1994). These studies are consistent with our results that Aβ42 induced a much stronger astroglial response than did Aβ40 (Figs. 1 and 2).

We also investigated whether neuron-derived soluble factor(s) may influence astrocytic responses to Aβ. This was addressed by treating astrocyte cultures with conditioned media from neuronal cultures previously treated with Aβ (see Section 2 for details). In rat astrocyte cultures, direct Aβ treatment increased GFAP expression significantly, and ApoE expression also increased with direct Aβ treatment (Figs. 3A and 4); ApoE expression, however, not significant. Furthermore, ApoE expression increased significantly in response to treatment with conditioned medium from cortical cultures exposed to Aβ for either 3 or 7 days (Figs. 3A and 4B). These results indicate that rat astrocytes themselves can be directly activated by Aβ and then increase ApoE expression, but expression of ApoE may be also influenced by an as of yet unidentified soluble factor(s) from neurons treated with Aβ. In monkey astrocyte cultures, only direct Aβ treatment increased both GFAP and ApoE expression, although the increase in GFAP was not significant (Figs. 3B and 4C,D). Similar to the case with rat astrocytes, monkey astrocytes can also be directly activated by Aβ. Unlike with rat astrocytes, ApoE expression in monkey astrocytes is only induced directly by Aβ. Thus, in the monkey brain, astrocytes may remove Aβ without requiring induction by neuronal signals, suggesting that possible species differences exist in the astrocytic responses to Aβ and in the mechanisms underlying these responses. From the study of cortical cultures, it was suggested that rat neuronal cells would be more sensitive to Aβ so that they may require a greater astroglial responses (Figs. 1 and 2D,E,I,J). ApoE is known to play a key role in lipid transport and metabolism, and is also important for neuronal repair (Poirier, 1994). Then rat astrocytes would be stimulated not only directly with Aβ but also by some soluble factors produced by neurons for much ApoE expression. On the other hand, it was also suggested that monkey neuronal cells would be more resistant to Aβ (Figs. 1 and 2D,E,I,J). Then monkey astrocytes would not need to express much ApoE such as rat. This may similarly occur in the human brain in which astrocytes may also be directly activated by Aβ. From these results, we concluded that astrocytes would be activated by Aβ in the early stages of Aβ accumulation and aggregation in the brain, during which time they remove excess Aβ before neurons can be damaged. Our conclusion is consistent with the findings that astrocytes are activated by Aβ, then take up Aβ for degradation (Funato et al., 1998; Matsunaga et al., 2003; Wyss-Coray et al., 2003), and that Aβ also induces astrocytes to produce ApoE and chemokines (Deb et al., 2003; LaDu et al., 2001; Smits et al., 2002). Taken together, these findings show that astroglia are in a pivotal position to reduce Aβ pathogenesis at an early stage, and thus may be a therapeutic target of great interest. Hence, additional studies will be required to clarify astroglial responses to Aβ.

In the present study, we also found species differences in the way astroglia respond to Aβ. Rat astrocytes were more sensitive to Aβ, and as such, may be a useful model to further investigate astroglial responses induced by Aβ. However, since the mechanism underlying the astroglial responses to Aβ was different in monkeys, and monkeys are phylogenetically more similar to humans, monkey cortical and astroglial cultures would be the models of choice to study potential therapeutic applications for humans.

Acknowledgements

The authors thank F. Ono and K. Terao of the Tsukuba Primate Center, National Institute of Infectious Diseases, Japan, for fetal cynomolgus monkey brain samples. This study was supported by a grant-in-aid from the Comprehensive Research on Aging and Health, Ministry of Health, Labor and Welfare, Japan.

References

Behl, C., Davis, J., Cole, G.M., Schubert, D., 1992. Vitamin E protects nerve cells from amyloid β protein toxicity. Biochem. Biophys. Res. Commun. 186, 944–952.

Burdick, D., Soreghan, B., Kwon, M., Kosmoski, J., Knauer, M., Henshen, A., Yates, J., Cotman, C., Glabe, C., 1992. Assembly and aggregation properties of synthetic Alzheimer's A4/beta amyloid peptide analogs. J. Biol. Chem. 267, 546–554.

Cardoso, S.M., Swerdlow, R.H., Oliviera, C.R., 2002. Induction of chytochrome c-mediated apoptosis by amyloid β 25-35 requires functional mitochondria. Brain Res. 931, 117–125.

Citron, M., Westaway, D., Xia, W., Carlson, G., Diehl, T., Levesque, G., Johnson-Wood, K., Lee, M., Seubert, P., Davis, A., Kholodensko, D., Motter, R., Sherrington, R., Perry, B., Yao, H., Strome, R., Lieberburg, I., Rommens, J., Kim, S., Schenk, D., Fraser, P., St. George-Hyslop, P., Selkoe, D.J., 1997. Mutant presenilins of Alzheimer's disease increase production of 42-residue amyloid beta-protein in both transfected cells and transgenic mice. Nature Med. 3, 67–72.

Deb, S., Zhang, J.W., Gottschall, P.E., 2003. β-Amyloid induces the production of active, matrix-degrading proteases in rat cultured rat astrocytes. Brain Res. 970, 205–213.

Funato, H., Yoshimura, M., Yamazaki, T., Saido, T.C., Ito, Y., Yokohujita, J., Okeda, R., Ihara, Y., 1998. Astrocytes containing amyloid beta-protein (Abeta)-positive granules are associated with Abeta40-positive diffuse plaques in the aged human brain. Am. J. Pathol. 152, 983–992.

Glenner, G.G., 1988. Alzheimer's disease: its proteins and genes. Cell 52, 307–308.

Ivins, K.J., Thornton, P.L., Rohn, T.T., Cotman, C.W., 1999. Neuronal apoptosis induced by beta-amyloid is mediated by caspase-8. Neurobiol. Dis. 6, 440–449.

Jarrett, J.T., Berger, E.P., Lansbury Jr., P.T., 1993. The carboxy terminus of the beta amyloid protein is critical for the seeding of amyloid formation: implications for the pathogenesis of Alzheimer's disease. Biochemistry 32, 4693–4697.

Koh, J., Yang, L.L., Cotman, C.W., 1990. β-amyloid protein increase the vulnerability of cultured cortical neurons to excitotoxic damage. Brain Res. 533, 315–320.

LaDu, M.J., Shah, J.A., Reardon, C.A., Getz, G.S., Bu, G., Hu, J., Guo, L., Van Eldik, L.J., 2001. Apolipoprotein E and apolipoprotein E receptors modulate Aβ-induced glial neuroinflammatory responses. Neurochem. Int. 39, 427–434.

Loo, D.T., Copani, A., Pike, C.J., Whittemore, E.R., Walencewicz, A.J., Cotman, C.W., 1993. Apoptosis is induced by β-amyloid in cultured central nervous system neurons. Proc. Natl. Acad. Sci. U.S.A. 90, 7951–7955.

Matsunaga, W., Shirokawa, T., Isobe, K., 2003. Specific uptake of Aβ 1-40 in rat brain occurs in astrocyte, but not in microglia. Neurosci. Lett. 342, 129–131.

Mattson, M.P., Cheng, B., Davis, D., Bryant, K., Lieberburg, I., Rydel, R., 1992. Beta-amyloid peptides destabilize calcium homeostasis and render human cortical neurons vulnerable to excitotoxicity. J. Neurosci. 12, 376–389.

Mattson, M.P., Partin, J., Begley, J.G., 1998. Amyloid beta-peptide induces apoptosis-related events in synapses and dendrites. Brain Res. 807, 167–176.

Morishima, Y., Gotoh, Y., Zieg, J., Barrett, T., Takano, H., Flavell, R., Davis, R.J., Shirasaki, Y., Greenberg, M.E., 2001. β-Amyloid induces neuronal apoptosis via a mechanism that involves the c-Jun n-terminal kinase pathway and the induction of Fas ligand. J. Neurosci. 21, 7551–7560.

Negishi, T., Ishii, Y., Kawamura, S., Kuroda, Y., Yoshikawa, Y., 2002a. Cryopreservation of brain tissue for primary culture. Exp. Anim. 51, 383–390.

Negishi, T., Ishii, Y., Kawamura, S., Kuroda, Y., Yoshikawa, Y., 2002b. Cryopreservation and primary culture of cerebral neurons from cynomolgus monkeys (*Macaca fascicularis*). Neurosci. Lett. 328, 21–24.

Negishi, T., Ishii, Y., Kyuwa, S., Kuroda, Y., Yoshikawa, Y., 2003. Primary culture of cortical neurons, type-1 astrocytes, and microglial cells from cynomolgus monkey (*Macaca fascicularis*) fetuses. J. Neurosci. Method 131, 133–140.

Poirier, J., 1994. Apolipoprotein E in animal models of CNS injury and in Alzheimer's disease. Trends Neurosci. 17, 525–530.

Selkoe, D.J., 1991. The molecular pathology of Alzheimer's disease. Neuron. 6, 487–498.

Smits, H.A., Rijsmus, A., Van Loon, J.H., Wat, J.W.Y., Verhoef, J., Boven, L.A., Nottet, H.S.L.M., 2002. Amyloid-β-induced chemokine production in primary human macrophages and astrocytes. J. Neuroimmnol. 127, 160–168.

Suzuki, N., Cheung, T.T., Cai, X.D., Odaka, A., Otvos Jr., L., Eckman, C., Golde, T.E., Younkin, S.G., 1994. An increased percentage of long amyloid beta protein secreted by familial amyloid beta protein precursor (beta APP717) mutants. Science 264, 1336–1340.

Takashima, A., Honda, T., Yasutake, K., Michel, G., Murayama, O., Murayama, M., Ishiguro, K., Yamaguchi, H., 1998. Activetion of tau protein kinase I/glycogen synthase kinase-3β by amyloid β peptide (25–35) enhances phosphorylation of tau in hippocampal neurons. Neuroscience Res. 31, 317–323.

Troy, C.M., Rabacchi, S.A., Friedman, W.J., Frappier, T.F., Brown, K., Shelanski, M.L., 2000. Caspase-2 mediates neuronal cell death induced by beta-amyloid. J. Neurosci. 20, 1386–1392.

Wyss-Coray, T., Loike, J.D., Brionne, T.C., Lu, E., Anankov, R., Yan, F., Silverstein, S.C., Husemann, J., 2003. Adult mouse astrocytes degrade amyloid-β in vitro and in situ. Nat. Med. 9, 453–457.

Yang, A.J., Chandswangbhuvana, D., Shu, T., Henschen, A., Glabe, C.G., 1999. Intracellular accumulation of insoluble, newly synthesized Aβn-42 in amyloid precursor protein-transfected cells that have been treated with Aβ1-42. J. Biol. Chem. 274 (29), 20650–20656.

Yankner, B.A., Duffy, L.K., Kirschner, D.A., 1990. Neurotrophic and neurotoxic effects of amyloid β protein: reversal by tachykinin neuropeptides. Science 25, 279–282.

Younkin, S.G., 1994. The amyloid beta protein precursor mutations linked to familial Alzheimer's disease alter processing in a way that fosters amyloid deposition. Tohoku J. Exp. Med. 174, 217–223.

Placenta (2005), 26, 99–103
doi:10.1016/j.placenta.2004.05.007

SHORT COMMUNICATION

Localization of Ubiquitin Carboxyl-terminal Hydrolase-L1 in Cynomolgus Monkey Placentas

S. Sekiguchi[a,*], A. Takatori[a], T. Negishi[a], J. Kwon[a,b], T. Kokubo[c], Y. Ishii[a], S. Kyuwa[a] and Y. Yoshikawa[a]

[a] Department of Biomedical Science, Graduate School of Agricultural and Life Sciences, University of Tokyo, 1-1-1 Yayoi, Bunkyo-ku, Tokyo 113-8657, Japan; [b] Department of Degenerative Neurological Disease, National Institute of Neuroscience, National Center of Neurology and Psychiatry, Kodaira, Tokyo 187-8502, Japan; [c] Fuji Photo Film Co., Ltd., Environmental Protection & Products Safety Division Material Safety Test Center, 210, Nakanuma, Minamiashigara-shi, Kanagawa 250-0193 Japan

Paper accepted 17 May 2004

Ubiquitin carboxyl-terminal hydrolase-L1 (UCH-L1) is a restrictedly expressed enzyme in neural and reproductive tissues, and it is considered to have a significant role in reproduction. In the present study, we investigated the localization of UCH-L1 in placenta of cynomolgus monkeys (*Macaca fascicularis*). UCH-L1 protein was detected in cytotrophoblasts of chorionic plate and villi, and decidual cells of decidua basalis in cynomolgus monkey placenta, and the amount of UCH-L1 protein in whole placenta increased as pregnancy progressed. These results supported that UCH-L1 is necessary for placental and fetal development in primate placenta. This is the first report to demonstrate the presence of UCH-L1 in primate placenta, and the cynomolgus monkey may be a useful model for the study of the functions of the ubiquitin–proteasome system in human pregnancy.
Placenta (2005), 26, 99–103

INTRODUCTION

The ubiquitin–proteasome system is a major pathway for protein degradation in eukaryotic cells [1]. This pathway uses the ubiquitin protein as a marker for intracellular protein processed by rapid proteolysis via a multi-subunit protease complex, the proteasome [2]. The ubiquitin-mediated degradation of certain regulatory proteins is considered to play a number of critical roles in cell-specific functions, including the cell cycle [3], apoptosis [4], inflammatory responses, and antigen presentation [5]. Attachment of ubiquitin to a target protein, referred to as ubiquitination, is a complex ATP-dependent process carried out by the ubiquitin-activating enzyme (E1), the ubiquitin-conjugating enzyme (E2) and ubiquitin ligase (E3) [6].

This pathway is considered to be important for placental growth and development. In previous studies, ubiquitin was detected in cytotrophoblasts in human placenta [7], and it has also been detected in decidual cells during pregnancy in the human uterus, although endometrial stromal cells in the non-pregnant uterus are known to have low concentrations of ubiquitin [8,9]. In vitro, human decidual cells have been shown to secrete ubiquitin [10]. In mice lacking the *UbcM4* gene encoding the E2 enzyme, multiple developmental abnormalities, such as a reduction in placental size, a thin chorionic plate, and scarce fetal blood vessels in the labyrinth, have been observed [11].

Ubiquitin carboxyl-terminal hydrolases (UCHs) are known to be de-ubiquitinating enzymes which recycle free ubiquitin from ubiquitin/protein complexes or polyubiquitin chains by cleaving the amide linkage neighboring the C-terminal glycine of ubiquitin [12]. UCH-L1, a member of the UCH family, is one of the most abundant soluble proteins in the brain (1–5% of the total soluble protein). Previous immunohistochemical studies have demonstrated that UCH-L1 is expressed exclusively in neuronal tissue [13–16], but it has also been reported in reproductive tissues such as spermatogonia and Sertoli cells in mice [15,17,18], spermatogonia in monkeys [19] and oocytes in mice [15]. Previous studies have also reported that gracile axonal dystrophy (gad) mutant mice, which lack UCH-L1, showed neuroaxonal dystrophy in the gracile nucleus of the medulla and the gracile fascicules of the spinal cord

* Corresponding author. Tel.: +81-3-5841-5038; fax: +81-3-5841-8186.
E-mail address: aa37162@mail.ecc.u-tokyo.ac.jp (S. Sekiguchi).

0143–4004/$–see front matter

[20–22]. In reproductive tissue, male gad mice exhibited a deterioration of spermatogenesis with aging [17]. Moreover, litter size in female gad mice was significantly lower than that in normal female mice, a finding which was independent of the genotype of the male partner [23]. We previously demonstrated the expression of UCH-L1 protein in decidual cells in the mouse placenta [24]. These results, when taken together, suggest that active UCH-L1 is necessary for normal reproductive processes to take place.

In the present study, we investigated the expression of UCH-L1, ubiquitin, and PCNA protein in the placenta of cynomolgus monkeys at three different gestational stages (50, 80, and 120 days of gestation), and we demonstrated the localization of UCH-L1 protein in cytotrophoblasts of the chorionic plate and villi, and in the decidual cells of the decidua basalis in the cynomolgus monkey placenta at all stages.

MATERIALS AND METHODS

Animals

Six pregnant cynomolgus monkeys (*Macaca fascicularis*) at gestational day (GD) 50, 80, and 120 ($n = 2$/each stage) were purchased from Shin Nippon Biomedical Laboratories, Ltd., and four monkeys at GD 83, 84, 93, and 102 were obtained from the Tsukuba Primate Center, National Institute of Infectious Diseases, Japan. The placentas were obtained by caesarean operation.

A piece of placenta at GD 50, 80, and 120 was fixed in 4% paraformaldehyde and embedded in paraffin for the immunohistochemical studies. The remaining placenta at GD 50, 80, and 120, as well as four whole placentas at GD 83, 84, 93, and 102 were subjected to Western blot analysis (see below).

Antibodies

A rabbit polyclonal antibody against protein gene product (PGP) 9.5 (PGP9.5; UltraClone Limited, England) was used for detecting UCH-L1. PGP 9.5 is equivalent to UCH-L1, and antibody against PGP 9.5/UCH-L1 is now widely used for investigation of the central and peripheral nervous systems. A rabbit polyclonal antibody against ubiquitin (Ubiquitin; DAKO, Denmark), and a mouse monoclonal antibody against proliferating cell nuclear antigen (PCNA; DAKO, Denmark) were used for detecting ubiquitin and proliferative activity of the cells, respectively.

Immunohistochemistry

Deparaffinized sections were pretreated with 0.3% H_2O_2 in methanol for 30 min for the inactivation of endogenous peroxidase and the sections were washed in phosphate buffer saline (PBS). Non-specific binding of immunoglobulins was blocked by incubation with Block Ace (Dainippon Pharmaceutical, Ltd., Japan) for 1 h at room temperature. The sections were then incubated with primary antibodies against PGP 9.5 (1:8000), ubiquitin (1:500), and PCNA (1:1000) for 16 h at 4 °C. The sections were then incubated with either biotinylated goat anti-rabbit or goat anti-mouse IgG (1:500; DAKO, Denmark), which was followed by incubation with streptavidin–biotin–horseradish peroxidase complex (sABC kit; DAKO, Denmark). The immunoreactive elements were visualized by treating the sections with 3,3′-diaminobenzidine tetroxide (Dojin Kagaku, Japan). Finally, the sections were counterstained with hematoxylin. The regions of placenta examined in this study included the chorionic plate, chorionic villi, cell columns, cytotrophoblastic shell, and decidua basalis. Negative control sections were incubated with non-immunized rabbit or mouse serum as substitutes for the primary antibody.

Western blot analysis

Placental tissue (5 g) was homogenized and fractionated into microsome fractions. The samples (20 μg of total protein) were electrophoresed by 15% SDS-PAGE. The separated proteins in the gels were transferred and blotted onto polyvinylidene fluoride membranes (Immobilon P; Millipore, Bedford, MA). After blocking the membranes with 5% nonfat dried milk in 20 mM phosphate buffer saline (pH 7.0) and 0.1% Tween-20 overnight at 4 °C, the blotted membranes were incubated with primary antibody (PGP 9.5; diluted at 1:15,000) for 1 h at room temperature. The membranes were then incubated with horseradish peroxidase conjugated goat anti-rabbit IgG (1:50,000, Jackson Lab, West Grove, PA) for 1 h at room temperature. Immunoreactions were visualized by enhanced chemiluminescence (ECL plus, Amersham, UK). Immunoreactive bands obtained from the Western blots were quantified using commercially available software (Quantity One; PDI, Upper Saddle River, NJ).

RESULTS

At all three stages, UCH-L1 protein was intensely and diffusely expressed in the cytoplasm and nuclei of the cytotrophoblasts of the chorionic plate and villi (Figure 1A–C). As regards the intensity of the immunoreaction of UCH-L1 in the cytotrophoblasts, no difference was observed among the three stages, but the number of chorionic villi increased markedly as the gestational days passed. At GD 50 and 80, ubiquitin protein was diffusely expressed in the cytoplasm and nuclei of the cytotrophoblasts and stromal cells, and only in the nuclei of the syncytiotrophoblasts of the chorionic villi (Figure 1D). At GD 120, ubiquitin protein was expressed in the cytoplasm and nuclei of the cytotrophoblasts and stromal cells, but only in the nuclei of syncytiotrophoblasts. PCNA protein was expressed in the cytotrophoblasts and stromal cells of the chorionic plate and villi at all three stages (data not shown).

UCH-L1 protein was not expressed in the cytotrophoblasts of the cell columns and cytotrophoblastic shell (Figure 1E and F), although ubiquitin protein was diffusely expressed in the cytoplasm and nuclei of the cytotrophoblasts at all three stages (Figure 1G and H). PCNA protein was expressed in the cytotrophoblasts in the cell columns and cytotrophoblastic shell at all three stages (Figure 1I and J).

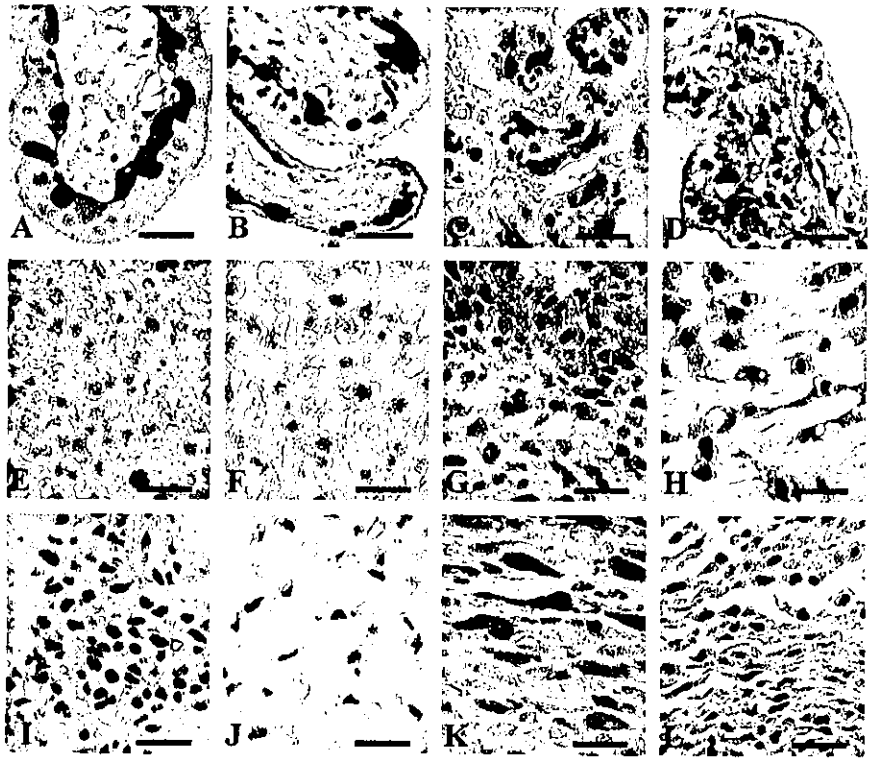

Figure 1. Immunohistochemistry of chorionic villi (A–D), cell columns (E, G and I), cytotrophoblastic shell (F, H and J) and decidua basalis (K and L) of cynomolgus monkey placenta against UCH-L1 (A–C, E, F and K), ubiquitin (D, G, H and L) and PCNA (I and J). UCH-L1 is detected in cytotrophoblasts of chorionic villi at gestational day (GD) 50 (A), 80 (B) and 120 (C), and in decidual cells at GD 80 (K), not in cytotrophoblasts of cell columns and cytotrophoblastic shell at GD 80 (E and F). Ubiquitin is detected in cytotrophoblasts, syncytiotrophoblasts and stromal cells of chorionic villi at GD 80 (D), cytotrophoblasts of cell columns and cytotrophoblastic shell at GD 80 (G and H), and decidua basalis at GD 80 (L). PCNA is detected in cytotrophoblasts of cell columns and cytotrophoblastic shell at GD 80 (I and J). Scale bar: 25 μm.

In the decidua basalis, UCH-L1 and ubiquitin protein were diffusely expressed in the cytoplasm and nuclei of decidual cells (Figure 1K and L). The intensity of the UCH-L1 immunoreaction in the decidual cells varied; these cells exhibited a mixed pattern at all three stages, i.e., some were intensely stained, while others were only slightly stained. The ubiquitin immunoreaction in the nuclei was more intense than in the cytoplasm of the decidual cells at all three stages. PCNA protein was expressed in the decidual cells at all three stages (data not shown).

Western blot analysis

Western blot analysis revealed that UCH-L1 protein was expressed in the placenta at all the stages of pregnancy (Figure 2A). The expression of UCH-L1 increased significantly ($p < 0.0001$) as pregnancy progressed (Figure 2B).

DISCUSSION

In the present study, we demonstrated the localization of UCH-L1 protein in the placenta of cynomolgus monkeys at three gestational stages for the first time. UCH-L1-, ubiquitin-, and PCNA-positive cytotrophoblasts were observed in the chorionic plate and villi at all stages.

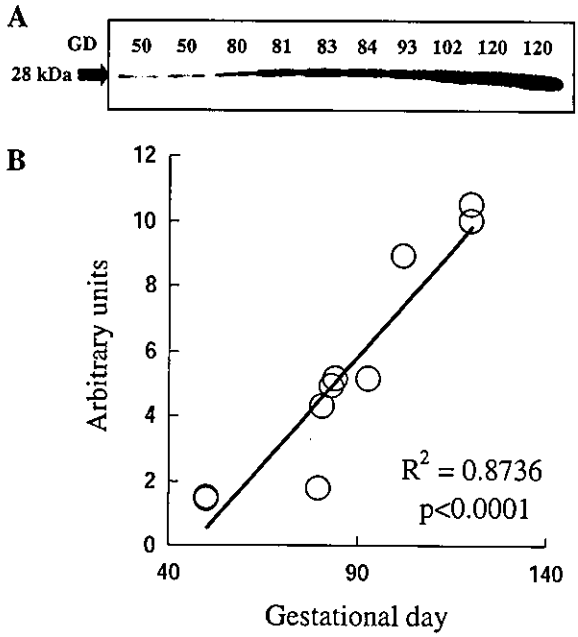

Figure 2. Analysis of UCH-L1 expression in cynomolgus monkey placentas. A 28 kDa band is detected in placentas at all gestational days (GD) (A). The expression of UCH-L1 increases significantly as pregnancy progresses (B).

Cytotrophoblasts of the chorionic plate and villi are essential for the exchange and passage of substances required for embryonic development [25], as well as for placental growth and development. For instance, ATP-binding cassette transporters such as P-glycoprotein (P-gp) and multidrug-resistance protein (MRP) have been shown to be localized in the brush-border membrane and the basement membrane of human placental trophoblasts and cytotrophoblasts also functioned as an efflux transport system for xenobiotics [26]. Also, this syncytial layer is thought to be the major placental barrier between maternal blood and fetal blood, although cytotrophoblasts can be an element of this barrier. Therefore, the localization of UCH-L1 and ubiquitin in the cytotrophoblasts of the chorion suggests that the ubiquitin–proteasome system creates the cell layer for the degradation of abnormal protein, which is exchanged or passed through the chorion. Furthermore, the localization of PCNA in cytotrophoblasts suggests that cytotrophoblasts are stem cells which proliferate rapidly and lead to placental growth. However, in the present study, cytotrophoblasts in the cell columns and cytotrophoblastic shell did not express UCH-L1, although they did express both ubiquitin and PCNA. Cytotrophoblasts in cell columns and cytotrophoblastic shell are known to play roles in infiltration and fixation into the decidua rather than exchanging substances and forming the blood–placenta barrier. Therefore, we suggest here that the ubiquitin–proteasome system in these areas functions with the aid of not UCH-L1, but rather other de-ubiquitinating enzymes.

The present study also determined the expression profiles of UCH-L1, ubiquitin, and PCNA in decidual cells in the decidua basalis of cynomolgus monkeys at three gestational phases. We previously investigated the expression of UCH-L1 protein in decidual cells of the mouse placenta, and our findings suggested that UCH-L1 plays a significant role in implantation and placental development [24]. Decidual cells, which are derived from endometrial stromal cells of the uterus following the establishment of pregnancy [9], play an important role in implantation and provide nutritional support for the embryo; they are also believed to protect the embryo from maternal immune rejection [27]. Therefore, we expect that the ubiquitin–proteasome system in decidual cells contributes to the degradation of unfavorable immunoproteins in order to enable fetal development.

In addition, the amount of UCH-L1 protein in the entire placenta increased in a stage-dependent manner. The number of chorionic villi increased in order to exchange or pass more effectively any necessary substances between mother and fetus with the passage of gestational days. Moreover, it was found that at GD 50, 80, and 120, the intensity and pattern of the UCH-L1 immunoreaction in the cytotrophoblasts remained unchanged. We considered that this finding was due to the increase in the number of UCH-L1-positive cytotrophoblasts, which occurred in concert with increments in the number of chorionic villi. The presence of UCH-L1 and the observed increase of the amount of UCH-L1 protein provide support for the idea that the contribution of the ubiquitin–proteasome system to fetal development increases as pregnancy progresses in primates.

In recent years, many studies have investigated placental function, as well as the developmental and reproductive toxicology of various toxic chemicals in rodents. However, rodents and primates have different gestation periods, and they also have different placental structures in the branches off the main projections of the chorionic plate. The primate placenta is of the villous type, and the chorionic villi maintain an arboreal pattern with innumerable branches. On the other hand, the branches off the main chorionic projections of the mouse labyrinth are much more interconnected and generate a maze-like pattern [28]. Thus, the intervillous space of primate placentas, which is filled with maternal blood, is more open than that of the mouse labyrinth. Although mouse placentas possess a three-layered labyrinth, primate placentas have double-layered chorionic villi, which are the analogue of the mouse labyrinth [28]. In our previous study, the mouse placenta was not found to have cytotrophoblasts stained with UCH-L1. Therefore, investigations of the rodent placenta may not accurately reflect human placental function. Thus, cynomolgus monkeys, which are non-human primates, could be a useful model for the further study of the various functions of the ubiquitin–proteasome system in human pregnancy.

In conclusion, we revealed the profiles of expression of UCH-L1 and ubiquitin protein in cytotrophoblasts and decidual cells. Our findings suggested that the ubiquitin–proteasome system is necessary for placental and fetal development in cynomolgus monkeys. In the future, further investigations of additional enzymes such as E1, E2, E3, proteasomes, and other de-ubiquitinating enzymes will be necessary to gain a better understanding of the role of the ubiquitin–proteasome system in the primate placenta.

REFERENCES

[1] Hochstrasser M. Ubiquitin, proteasomes, and the regulation of intracellular protein degradation. Curr Opin Cell Biol 1995;7:215–23.
[2] Adams J. The proteasome: structure, function, and role in the cell. Cancer Treat Rev 2003;29:3–9.
[3] Naujokat C, Hoffmann S. Role and function of the 26S proteasome in proliferation and apoptosis. Lab Invest 2002;82:965–80.
[4] Yang Y, Yu X. Regulation of apoptosis: the ubiquitous way. FASEB J 2003;17:790–9.
[5] Rock KL, Goldberg AL. Degradation of cell proteins and the generation of MHC class I-presented peptides. Annu Rev Immunol 1999;17:739–79.
[6] Baek KH. Conjugation and deconjugation of ubiquitin regulating the destiny of proteins. Exp Mol Med 2003;35:1–7.
[7] Bebington C, Doherty FJ, Fleming SD. Ubiquitin and ubiquitin–protein conjugates are present in human cytotrophoblast throughout gestation. Early Pregnancy 2000;4:240–52.
[8] Bebington C, Doherty FJ, Fleming SD. The possible biological and reproductive functions of ubiquitin. Hum Reprod Update 2001;7:102–11.
[9] Bebington C, Bell SC, Doherty FJ, Fazleabas AT, Fleming SD. Localization of ubiquitin and ubiquitin cross-reactive protein in human and baboon endometrium and decidua during the menstrual cycle and early pregnancy. Biol Reprod 1999;60:920–8.
[10] Ren SG, Braunstein GD. Production of superoxide dismutase, beta 2-microglobulin and ubiquitin by human term decidua in vitro. Early Pregnancy 1995;1:124–9.

[11] Harbers K, Muller U, Grams A, Li E, Jaenisch R, Franz T. Provirus integration into a gene encoding a ubiquitin-conjugating enzyme results in a placental defect and embryonic lethality. Proc Natl Acad Sci U S A 1996;93:12412–7.

[12] Wilkinson KD, Deshpande S, Larsen CN. Comparisons of neuronal (PGP 9.5) and non-neuronal ubiquitin C-terminal hydrolases. Biochem Soc Trans 1992;20:631–7.

[13] Schofield JN, Day IN, Thompson RJ, Edwards YH. PGP9.5, a ubiquitin C-terminal hydrolase; pattern of mRNA and protein expression during neural development in the mouse. Brain Res Dev Brain Res 1995;85: 229–38.

[14] Kent C, Clarke PJ. The immunolocalisation of the neuroendocrine specific protein PGP9.5 during neurogenesis in the rat. Brain Res Dev Brain Res 1991;58:147–50.

[15] Wilson PO, Barber PC, Hamid QA, Power BF, Dhillon AP, Rode J, et al. The immunolocalization of protein gene product 9.5 using rabbit polyclonal and mouse monoclonal antibodies. Br J Exp Pathol 1988;69: 91–104.

[16] Wilkinson KD, Lee KM, Deshpande S, Duerksen-Hughes P, Boss JM, Pohl J. The neuron-specific protein PGP 9.5 is a ubiquitin carboxyl-terminal hydrolase. Science 1989;246:670–3.

[17] Kwon J, Kikuchi T, Setsuie R, Ishii Y, Kyuwa S, Yoshikawa Y. Characterization of the testis in congenitally ubiquitin carboxy-terminal hydrolase-1 (Uch-L1) defective (gad) mice. Exp Anim 2003;52:1–9.

[18] Kon Y, Endoh D, Iwanaga T. Expression of protein gene product 9.5, a neuronal ubiquitin C-terminal hydrolase, and its developing change in Sertoli cells of mouse testis. Mol Reprod Dev 1999;54:333–41.

[19] Tokunaga Y, Imai S, Torii R, Maeda T. Cytoplasmic liberation of protein gene product 9.5 during the seasonal regulation of spermatogenesis in the monkey (*Macaca fuscata*). Endocrinology 1999; 140:1875–83.

[20] Yamazaki K, Wakasugi N, Tomita T, Kikuchi T, Mukoyama M, Ando K. Gracile axonal dystrophy (GAD), a new neurological mutant in the mouse. Proc Soc Exp Biol Med 1988;187:209–15.

[21] Saigoh K, Wang YL, Suh JG, Yamanishi T, Sakai Y, Kiyosawa H, et al. Intragenic deletion in the gene encoding ubiquitin carboxy-terminal hydrolase in gad mice. Nat Genet 1999;23:47–51.

[22] Ichihara N, Wu J, Chui DH, Yamazaki K, Wakabayashi T, Kikuchi T. Axonal degeneration promotes abnormal accumulation of amyloid beta-protein in ascending gracile tract of gracile axonal dystrophy (GAD) mouse. Brain Res 1995;695:173–8.

[23] Yamazaki K, Wakasugi N, Sakakibara A, Tomita T. Reduced fertility in gracile axonal dystrophy (gad) mice. Jikken Dobutsu 1988;37: 195–9.

[24] Sekiguchi S, Yoshikawa Y, Tanaka S, Kwon J, Ishii Y, Kyuwa S, et al. Immunohistochemical analysis of protein gene product 9.5, a ubiquitin carboxyl-terminal hydrolase, during placental and embryonic development in the mouse. Exp Anim 2003;52:365–9.

[25] Knipp GT, Audus KL, Soares MJ. Nutrient transport across the placenta. Adv Drug Deliv Rev 1999;38:41–58.

[26] Nagashige M, Ushigome F, Koyabu N, Hirata K, Kawabuchi M, Hirakawa T, et al. Basal membrane localization of MRP1 in human placental trophoblast. Placenta 2003;24:951–8.

[27] Fazleabas AT, Strakova Z. Endometrial function: cell specific changes in the uterine environment. Mol Cell Endocrinol 2002;186:143–7.

[28] Georgiades P, Ferguson-Smith AC, Burton GJ. Comparative developmental anatomy of the murine and human definitive placentae. Placenta 2002;23:3–19.

BIOLOGY OF REPRODUCTION 71, 515–521 (2004)
Published online before print 14 April 2004.
DOI 10.1095/biolreprod.104.027565

Developmental Regulation of Ubiquitin C-Terminal Hydrolase Isozyme Expression During Spermatogenesis in Mice

Jungkee Kwon,[2,3] Yu-Lai Wang,[1] Rieko Setsuie,[3,4] Satoshi Sekiguchi,[2] Mikako Sakurai,[3,4] Yae Sato,[3,4] Won-Woo Lee,[2] Yoshiyuki Ishii,[2] Shigeru Kyuwa,[2] Mami Noda,[4] Keiji Wada,[3] and Yasuhiro Yoshikawa[1,2]

Department of Biomedical Science,[2] Graduate School of Agricultural and Life Sciences, University of Tokyo, Bunkyo-ku, Tokyo, 113-8657, Japan
Department of Degenerative Neurological Disease,[3] National Institute of Neuroscience, National Center of Neurology and Psychiatry, Kodaira, Tokyo, 187-8502, Japan
Laboratory of Pathophysiology,[4] Graduate School of Pharmaceutical Sciences, Kyushu University, Higashi-ku, Fukuoka, 812-8582, Japan

ABSTRACT

The ubiquitin pathway functions in the process of protein turnover in eukaryotic cells. This pathway comprises the enzymes that ubiquitinate/deubiquitinate target proteins and the proteasome that degrades ubiquitin-conjugated proteins. Ubiquitin C-terminal hydrolases (UCHs) are thought to be essential for maintaining ubiquitination activity by releasing ubiquitin (Ub) from its substrates. Mammalian UCH-L1 and UCH-L3 are small proteins that share considerable homology at the amino acid level. Both of these UCHs are highly expressed in the testis/ovary and neuronal cells. Our previous work demonstrated that UCH-L1-deficient gracile axonal dystrophy (*gad*) mice exhibit progressively decreasing spermatogonial stem cell proliferation, suggesting that UCH isozymes in the testis function during spermatogenesis. To analyze the expression patterns of UCH isozymes during spermatogenesis, we isolated nearly homogeneous populations of spermatogonia, spermatocytes, spermatids, and Sertoli cells from mouse testes. Western blot analysis detected UCH-L1 in spermatogonia and Sertoli cells, whereas UCH-L3 was detected in spermatocytes and spermatids. Moreover, reverse transcription-polymerase chain reaction analysis of UCH isozymes showed that UCH-L1 and UCH-L4 mRNAs are expressed in spermatogonia, whereas UCH-L3 and UCH-L5 mRNAs are expressed mainly in spermatocytes and spermatids. These results suggest that UCH-L1 and UCH-L3 have distinct functions during spermatogenesis, namely, that UCH-L1 may act during mitotic proliferation of spermatogonial stem cells whereas UCH-L3 may function in the meiotic differentiation of spermatocytes into spermatids.

male reproductive tract, meiosis, Sertoli cells, spermatogenesis, testis

INTRODUCTION

Ubiquitination of proteins is mediated by specific enzymes, namely E1 (ubiquitin-activating), E2 (ubiquitin-conjugating), and E3 (ubiquitin ligase) [1]. In this pathway, polyubiquitinated proteins are translocated to the proteasome and proteolytically degraded in an energy-dependent manner. The ubiquitin pathway plays important roles in regulating numerous cellular processes, including the degradation of intracellular proteins, cell-cycle regulation, stress responses, and programmed cell death [2–6]. Ubiquitin can be released from polyubiquitin chains or ubiquitin-protein conjugates via the action of deubiquitinating enzymes. These enzymes are divided into two families: ubiquitin C-terminal hydrolases (UCHs) and ubiquitin-specific proteases (UBPs). UCHs remove ubiquitin from peptides or small C-terminal ubiquitin adducts only, whereas UBPs are thought to disassemble polyubiquitin chains [7, 8].

Recent studies show that there are at least four mammalian UCH isozymes, among which the residues surrounding the active site share a high degree of homology [8, 9]. Mouse *Uchl1* and *Uchl3* encode proteins of similar size that share 52% amino acid sequence identity [8, 10]. However, the distribution of these isozymes is quite distinct; UCH-L1 mRNA is selectively and highly expressed in the testis/ovary and neuronal cells [10–12], whereas UCH-L3 mRNA is expressed in all tissues, including the testis/ovary and brain [13, 14]. UCH-L1-specific antibodies stain the testis, especially spermatogonia and Sertoli cells [15–18]. In addition, UCH-L1-deficient gracile axonal dystrophy (*gad*) mutant mice exhibit pathological changes, such as progressively decreasing spermatogonial stem cell proliferation [18]. These results led us to postulate that UCH isozymes in the testis function in the development of spermatogonia into mature sperm. Spermatogenesis is a complex, highly organized process that is divided into three phases: proliferation, meiosis, and spermiogenesis [19], each of which may require the activity of specific UCH isozymes. However, our understanding of the functional roles and the localization of UCH isozymes during spermatogenesis is limited.

In the present study, we generated peptide-specific antibodies against sequences within UCH-L1 or UCH-L3 and purified developing sperm cells at each stage from testes using immunomagnetic beads followed by discontinuous Percoll gradient centrifugation [20–23]. We found that the expression level of each UCH isozyme increased during the first round of spermatogenesis, and that the isozymes exhibited differential expression in the mouse testis [24]. Our results suggest that UCH isozymes play an important role in the regulation of spermatogenesis.

[1]Correspondence: Yasuhiro Yoshikawa, Department of Biomedical Science, Graduate School of Agricultural and Life Sciences, University of Tokyo, 1-1-1 Yayoi, Bunkyo-ku, Tokyo 113-8657, Japan.
FAX: 81 3 5841 8186; e-mail: ayyoshi@mail.ecc.u-tokyo.ac.jp

Received: 20 January 2004.
First decision: 5 February 2004.
Accepted: 19 March 2004.

ISSN: 0006-3363. http://www.biolreprod.org

MATERIALS AND METHODS

Animals

The *gad* [11] and *Uchl3* knockout [13] mice were used as controls. The *gad* mouse is an autosomal recessive mutant that was obtained from the cross between CBA and RFM mice. The mutant line was maintained by intercross for more than 20 generations. The *Uchl3* knockout mouse was generated by the standard method using homologously recombinant ES cells from 129SV mice. The knockout line was back-crossed several times to C57BL/6J mice. Male Balb/c mice were purchased from Nihon CLEA, Inc. (Tokyo, Japan), and all animals were maintained at the National Institute of Neuroscience, National Center of Neurology and Psychiatry (Japan).

All mouse experiments were performed in accordance with the institution's regulations for animal care and with the approval of the Animal Investigation Committee.

Isolation of Type A Spermatogonia and Sertoli Cells

Sequential enzymatic digestion of testicular tubules was performed as previously described [21]. After treatment with erythrocyte lysing buffer, testes from ten 2-wk-old and two 8-wk-old Balb/c mice were incubated twice for 5 min at 34°C with medium containing 0.5 mg/ml collagenase IV-S (Sigma-Aldrich, St. Louis, MO) and digested for 10 min at 34°C with medium containing 1 mg/ml trypsin (Sigma-Aldrich).

After the sequential enzymatic digestion, type A spermatogonia were isolated using immunomagnetic beads. The cells were incubated at room temperature for 15 min with biotin-conjugated rat anti-mouse CD117 (1 μg/10^6 cells), which recognizes the extracellular domain of the c-kit receptor (clone 2B8; Pharmingen, San Diego, CA). The cell suspension was then centrifuged at 300 × *g* for 5 min and washed with Dulbecco modified Eagle medium to remove excess antibody. The cell pellet was then resuspended in 80 μl buffer and incubated with 20 μl MACS anti-biotin microbeads (Miltenyi Biotec, Bergisch Gladbach, Germany) per 10^7 total cells at 6–12°C for 15 min. The cell suspension was then washed carefully and resuspended in 500 μl buffer per 10^8 total cells. The c-kit-positive cells (type A spermatogonia) were separated with a MACS separator (Miltenyi Biotec) and collected. The suspension containing Sertoli cells was resuspended at a concentration of 1 × 10^6 cells/ml in tissue culture medium containing 10% fetal calf serum.

Sertoli Cell Culture and Purification

The suspension containing Sertoli cells obtained from testes of ten 2-wk-old mice was plated on lectin- (Datura stramonium agglutinin; Sigma, St. Louis, MO) coated dishes as described [25, 26] and incubated for 3 days at 37°C. Alkaline phosphatase activity was visualized according to the procedure of Cox and Singer [27]. Cultured cells were incubated in reaction buffer (100 mM Tris-HCl, 100 mM NaCl, 50 mM $MgCl_2$, pH 9.5) containing 0.17 mg/ml 5-bromo-4-chloro-3-indolyl phosphate and 0.33 mg/ml nitro blue tetrazolium chloride.

Isolation of Spermatocytes and Spermatids

After isolating type A spermatogonia from testes of 8-wk-old mice using immunomagnetic beads, the testicular cell suspension was separated by discontinuous Percoll (Amersham Biosciences, Piscataway, NJ) gradient centrifugation [20]. The recovered cell populations were analyzed by phase-contrast microscopy [28], fluorescence-activated cell sorting (FACS) [29], and reverse transcription-polymerase chain reaction (RT-PCR).

RT-PCR Analysis of Isolated Cells Expressing Specific Marker Genes

From each population of spermatogonia, spermatocytes, spermatids, and Sertoli cells isolated from testicular cell suspensions, mRNAs were extracted using the QuickPrep micro mRNA purification kit (Amersham Biosciences) and subjected to reverse transcription with a first-strand cDNA synthesis kit (Amersham Biosciences) according to the manufacturer's instructions. PCR was performed with the following primers; c-kit [30], 5′-AAGATTTGCGATTTCGGGC-3′ and 5′-CTGAAAATGCTCTC TGGTGCC-3′; Histone H1t [7], 5′-GTCCAGCTCTTGACCATGTCG-3′ and 5′-GCTTTTTCCCTCGCCTTTTAG-3′; SP-10 [31], 5′-TTTATCTG CTTGGATCTGCCC-3′, and 5′-GCTTGAAAGTTGCTGAACCG-3′; stem cell factor (SCF) [32], 5′-ATAGGAAAGCCGCAAAGGC-3′ and 5′-TTACAAGCGAAATGAGAGCCG-3′; and glyceraldehyde-3-phosphate dehydrogenase [33]. Each sample was amplified using the AmpliTaq Gold GeneAmp system (Applied Biosystems, Foster City, CA).

FACS Analysis of Isolated Cells

FACS analysis was performed as described by Malkove et al. [29, 34]. Briefly, isolated spermatogenic cells were fixed in 70% ethanol overnight at 4°C and then incubated in propidium iodide staining solution (50 μg/ml and 100 U/ml RNase A in PBS) for 30 min at room temperature. Within 2 h poststaining, the isolated spermatogenic cells were analyzed by FACS (FACSCalibur, Becton Dickinson, Franklin Lakes, NJ). Excitation was at 488 nm and emission was at ~600 nm.

Quantitative mRNA Analysis of UCH Isozyme Genes by Real-Time PCR

SYBR Green-based real-time quantitative RT-PCR (ABI PRISM 7700 Sequence detection system, Columbia, MD) was performed [33, 35] in SYBR Green Master mix using the following primers; UCH-L1, 5′-TTCTGTTCAACAACGTGGACG-3′ and 5′-TCACTGGAAAGGGCAT TCG-3′; UCH-L3, 5′-TGAAGGTCAGACTGAGGCACC-3′ and 5′-AA TTGGAAATGGTTTCCGTCC-3′; UCH-L4, 5′-AAACAAACCATCAG CAATGCC-3′ and 5′-GACCCTGATTCAAAGTGCACC-3′; UCH-L5, 5′-TTTTCTTTTCAAGTGGCAGCC-3′ and 5′-GATAGCCTGAGTGGC ACAAGC-3′; and β-actin, 5′-CGTGCGTGACATCAAAGAGAA-3′ and 5′-CAATAGTGATGACCTGGCCGT-3′. For comparing relative UCH isozyme gene expression in isolated germ cells and Sertoli cells, the formula 2^{-ddCt} was used to calculate relative expression levels compared with spermatogonia of two-week-old mice. For comparing the expression level of UCH isozyme genes in the time course of testicular maturation, the formula 2^{-ddCt} was used to calculate relative expression levels compared with the testes of 5-day-old mice.

Western Blotting of UCH-L1 and UCH-L3 from Isolated Cells

Total protein was extracted [24] from isolated testicular cells or whole testes of 5-, 7-, 15-, 19-, 21-, 23-, 26-, and 33-day-old Balb/c mice. Control extracts were obtained from testes of *gad* and *Uchl3* knockout mice. For preparation of antibodies, we designed two specific peptides, AQHEN-FRKKQIEELKGQEVSPK (R891A, GenBank no. NP_057932, residues 57–78) and EKYEVFRTEEEEKIKSQGQDVTSS (R837A, GenBank no. NP_035800, residues 60–83) corresponding to mouse UCH-L1 and UCH-L3, respectively. Polyclonal antibodies against R891A and R837A were raised in rabbits and the IgG fraction was isolated (Tana Laboratories, L.C., Houston, TX). Each sample was adjusted to 5 μg protein/10 μl and subjected to SDS-PAGE (15% acrylamide; XV Pantera gel; DRC, Tama, Japan). After transferring the proteins to a nitrocellulose membrane and blocking with 5% skim milk, the membranes were incubated at 4°C overnight with the primary antibody to UCH-L1 (1:1000) or UCH-L3 (1:400). The membranes were then incubated with peroxidase-conjugated goat anti-rabbit IgG (H+L) (1:10 000; Pierce, Rockford, IL) for 60 min at room temperature. Immunoreactivity was visualized using the SuperSignal detection kit (Pierce) and analyzed with a ChemiImager (Alpha Innotech, San Leandro, CA).

Immunohistochemistry of UCH-L1 and UCH-L3

Tissues were fixed in vivo with 4% paraformaldehyde in phosphate-buffered saline (PBS) and embedded in paraffin, and sections (4 μm thickness) were treated with absolute methanol containing 3% H_2O_2 for 30 min to block endogenous peroxidase activity. After blocking with 10% goat serum for 1 h at room temperature, the sections were incubated at 4°C overnight with antibodies to UCH-L1 (1:500) or UCH-L3 (1:200) diluted in PBS containing 1% BSA. The sections were then incubated with fluorescein isothiocyanate-conjugated anti-rabbit IgG (1:200, Jackson ImmunoResearch, West Grove, PA) for 1 h at room temperature and examined by confocal laser scanning microscopy (Olympus, Tokyo, Japan).

RESULTS

Isolation of Spermatogenic Cells and Sertoli Cells

Using the c-kit antibody, we isolated an average of 17 × 10^5 type A spermatogonia from ten 2-wk-old juvenile mice and an average of 3.5 × 10^5 type A spermatogonia